Progress of Theoretical Physics, Vol. 105, No. 1, January 2001

Fermionic Renormalization Group Flows

— *Technique and Theory* —

Manfred Salmhofer[1] and Carsten Honerkamp[2]

[1] *Mathematik, ETH-Zentrum, 8092 Zürich, Switzerland*
[2] *Theoretische Physik, ETH-Hönggerberg, 8093 Zürich, Switzerland*

(Received November 7, 2000)

We give a self-contained derivation of the differential equations for Wilson's renormalization group for the one-particle irreducible Green functions in fermionic systems. The application of this equation to the (t, t')-Hubbard model appears in Ref. 9). Here we focus on theoretical aspects. After deriving the equations, we discuss the restrictions imposed by symmetries on the effective action. We discuss scaling properties due to the geometry of the Fermi surface and give precise criteria to determine when they justify the use of one-loop flows. We also discuss the relationship of this approach to other RG treatments, as well as aspects of the practical treatment of truncated equations, such as the projection to the Fermi surface and the calculation of susceptibilities.

§1. Introduction

Renormalization group (RG) studies of fermionic models are important for understanding models of solid-state theory and high-energy physics. In this paper, we set up a system of equations suitable for studying flows for general fermionic systems, in particular those with a Fermi surface at any density, and discuss general, but nontrivial, properties of their solutions. The system of equations applies both to "normal" and to symmetry-broken situations of fermionic systems with short-range interactions for $d \geq 1$. By "short-range" we mean that the two-particle interaction decays so fast that its Fourier transform is a regular function. In Ref. 9) we have, together with Furukawa and Rice, applied the RG equations that we derive here to the two-dimensional (t, t')-Hubbard model in the regime relevant for high-temperature superconductivity. The purpose of the present paper is to give more background on the theoretical aspects of the equations, in particular on a detailed argument which justifies the one-loop flow in a certain scale range, even if the scale-dependent interaction is no longer small. In the following, we give an overview; the details are filled in in the later sections.

1.1. *The RG and the three scale regimes*

The Wilsonian RG organizes the functional integration corresponding to the grand canonical trace as an iterated integral over degrees of freedom with energies in a certain range, i.e. those that belong to a corresponding length scale. As such, it is simply a rewriting of the generating functional of the correlation functions as a function of an energy scale ϵ. In contrast to the situation in other RG schemes, this approach does not require any assumptions about perfect scaling laws as a

function of ϵ. This idea of integrating over some degrees of freedom does not a priori require a splitting of the Hamiltonian into a term describing free particles and an interaction term, with an assumption that the interaction term is small. However, it is of course in general a very difficult task to calculate renormalization group flows in strongly coupled systems, and we assume that the interaction in the Hamiltonian, which plays the role of the initial interaction, is weak, so that we can think of energy scales as *kinetic* energy scales. Thus the method we describe here is a weak-coupling technique. A well-known property of the effective interaction is that it cannot be described by a single coupling constant, and in the cases we are interested in, we need to study a coupling function that depends on the momenta of the particles, as well as on the energy scale ϵ. As the energy scale ϵ decreases, the generic behaviour in two or more spatial dimensions is that the coupling function grows. Thus, even with a weak initial interaction, the flow eventually leaves the weak-coupling regime, unless the temperature is above all critical temperatures, so that any instabilities are prevented (see Ref. 2) and the discussion below). This growth of the effective interaction signals instabilities, and from the technical point of view it means that one has to switch to a different description of the system, e.g. in terms of composite fields describing Cooper pairs or spin variables. Because of the semigroup property of the RG flow (which we recall in §2.2), one can stop the flow at a nonzero scale ϵ_2 and rewrite the effective interaction in terms of the new fields at that scale. However, in the context of the present method, the first question is to what scale one can get using the weak-coupling flow. In §5 we give a precise criterion to determine how large the coupling constants are allowed to become before the corrections to the one-loop flow become significant. It turns out that there are nontrivial effects that suppress these corrections even if the couplings are no longer small, and these effects depend on the geometry of the Fermi surface. In the following, we briefly describe the main idea behind a picture of three scale regions.

The renormalization group defines an effective interaction for the fermions with kinetic energy $e(\boldsymbol{p})$ less than some ϵ, obtained from the original interaction of the model by integrating over the degrees of freedom with energies greater than ϵ. (In the technical implementation, it is useful to use smooth cutoff functions.) The phase space $\{\boldsymbol{p} : |e(\boldsymbol{p})| \leq \epsilon\}$ of the fermions with energy at most ϵ is a neighbourhood of the Fermi surface. Thus the shape of the Fermi surface determines the low-energy phase space, and this essentially determines which terms are dominant in the RG equations. If the Fermi surface is curved, there are power counting gains that suppress contributions from all graphs that have overlapping loops. This is made precise by an inequality for integrals of two or more loops that gives a rigorous bound for such integrals.[11),12),14)] The constants in this bound depend on the curvature of the Fermi surface, and they diverge when the curvature of the Fermi surface vanishes. As shown in Refs. 11) and 2), the only four-legged graphs that do not have overlapping loops are generated by the one-loop RG equation. This implies that there is an energy scale ϵ_1, *determined by the curvature of the Fermi surface*, below which "overlapping loop" effects[11)] produce small scale factors that suppress corrections to the one-loop flow. Thus, below this energy scale, one has an argument for the validity of the one-loop flow, which does not require coupling constants to be

very small (see §5).

The flow thus splits in a natural way into three energy scale regions as follows. Regime 1 contains the high scales, with energy above ϵ_1. In this regime, the only justification of a weak-coupling treatment is that the coupling constants are indeed small, so that higher order terms are small. On the other hand, this justification is mathematically rigorous: because the energy scale ϵ_1 provides an infrared cutoff for the functional integral for the effective action at scale ϵ_1, and because the fields are fermionic, there are rigorous proofs [13] that the perturbation expansion for the effective action at scale ϵ_1 converges. Thus perturbation theory can be used to calculate the effective action at scale ϵ_1 reliably, if the coupling is smaller than a value that depends on ϵ_1.

Regime 2 is below ϵ_1. Here, the scaling improvements due to overlapping loops now supress corrections to the one-loop flow. The latter usually gives growing coupling constants, especially in physically interesting cases. This signals the tendency toward (possibly competing) instabilites. However, the scaling improvements due to overlapping loops are sufficiently strong to suppress the corrections to the one-loop flow, even when the coupling constants are no longer small. The one-loop flow itself leads to a divergence of the coupling constants at a certain scale ϵ^*. Thus, for $\epsilon_2 > \epsilon^*$, the coupling constants become so large that the scaling improvements are insufficient to suppress the large factor from the coupling constants, and then the one-loop approximation breaks down. The scales ϵ_1 and ϵ_2 will be determined in detail in §5 (see in particular Eq. (111)).

Regime 3 is below ϵ_2. Here, the theory is strongly coupled. However, the interaction changes — and if usually simplified — during the flow. For instance, in the superconducting case, a leading term has emerged which corresponds to the BCS model. In the (t, t')-Hubbard model, the interaction also develops a pronounced k-space structure at that scale, [9] which may lead to a tractable theory, but a full strong-coupling theory has not yet been developed.

In summary, if one starts out at weak coupling, the one-loop RG flow is justified down to an energy scale ϵ_2, which is determined by the curvature of the Fermi surface, and at which the effective coupling function need no longer be small. The details of the flow down to the scale ϵ_2 depend on the shape of the Fermi surface, as well as on the strength of the initial coupling constant. We give a brief discussion of some cases in the next subsection.

1.2. *Some consequences*

1.2.1. The Kohn-Luttinger effect

In the case that the Fermi surface is positively curved and in which Umklapp scattering is irrelevant, the three-scale picture provides a simple view of the Kohn-Luttinger effect at weak coupling. Because the Fermi surface is curved, the particle-hole terms in the flow equation (67) are small compared to the particle-particle terms. The leading part of the coupling function is then obtained by projecting on the Fermi surface, and one can expand the coupling function in an orthonormal basis of functions ϕ_l on the Fermi surface. The particle-particle flow has the property that it decouples different l, so that the corresponding coupling constants g_l all flow

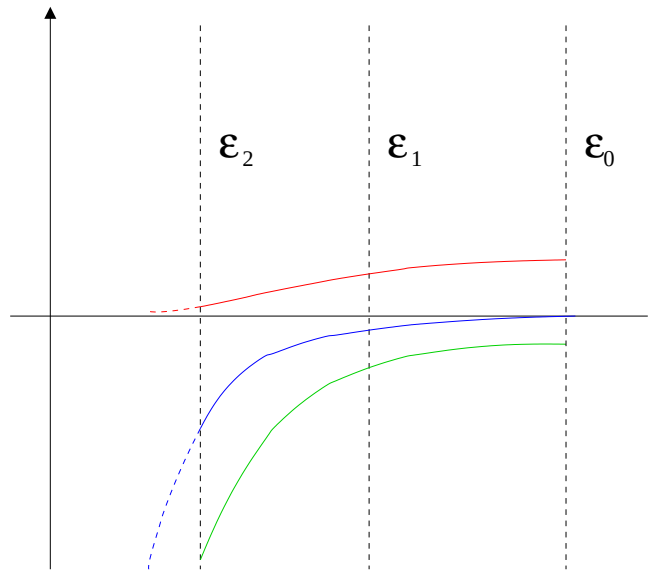

Fig. 1. The three scales and the flow of some coupling constants. The flow starts at the scale ϵ_0. Below the scale ϵ_1, but above the scale ϵ_2, scaling effects from overlapping loops justify a one-loop flow even if the couplings are not small. The flow of the coupling constants is sketched for the situation without Umklapp scattering and in which the particle-particle term dominates the flow. In this case, couplings that are negative grow in absolute value, and positive couplings are suppressed. Below the scale ϵ_2, the one-loop flow can no longer be justified.

independently, according to the equations

$$\dot{g}_l = -\tilde{\beta}_l g_l^2. \tag{1}$$

(For a more detailed discussion, see Ref. 3), §4.5.) Because (1) is only accurate below ϵ_1, the initial condition for the g_l is given at the scale ϵ_1. If a given g_l is a repulsive coupling at ϵ_1, i.e. $g_l(\epsilon_1) > 0$, then g_l decreases as ϵ decreases. If a given g_l is an attractive coupling at ϵ_1, i.e. $g_l(\epsilon_1) < 0$, then g_l increases in absolute value (see Fig. 1). The Kohn-Luttinger effect is the observation that for a weak repulsive interaction at scale ϵ_0, there are values of l for which g_l is negative at the lower scale ϵ_1, and thus it becomes larger in absolute value below that scale (see Fig. 1), eventually leading to a superconducting state with the gap symmetry given by l.

Because the maximal four-point function defined in §5 initially grows at most logarithmically in the energy scale, renormalized perturbation theory above the scale ϵ converges if the largest initial coupling constant g_0 at the scale ϵ_0 satisfies the

inequality $|g_0| \log \epsilon_0/\epsilon \ll 1$. (Here "renormalized" means that the Fermi surface shift is treated appropriately.[11),12)])

Thus, if $|g_0| \log \epsilon_0/\epsilon_1 \ll 1$, one can determine the superconducting instabilities of the weak-coupling model by performing a perturbative calculation to determine the g_l at the scale ϵ_1 and checking which of these coupling constants is the most negative.

It is important to note that the above-mentioned decoupling of the flow of the coupling constants g_l holds only in absence of Umklapp scattering and when the particle-hole diagrams are not singular. (This requires in particular the absence of van Hove singularities.) If the particle-hole terms in the flow are important, the above-mentioned expansion in Fermi surface harmonics ϕ_l does not lead to decoupled flow equations. This, and the Umklapp scattering, is physically very important in the (t, t')-Hubbard model (see Refs. 16) and 9) and the references therein).

1.2.2. Small curvature and nesting effects

The Kohn-Luttinger effect always drives the system to a superconducting state if the coupling function remains small down to the scale where the particle-particle flow is leading. As discussed above, such a scale always exists if the Fermi surface is curved, but it goes to zero when the curvature goes to zero. By the above reasoning, if the curvature of the Fermi surface is nonzero, one can make the initial coupling constant sufficiently small that one stays in the weak-coupling regime down to the scale where the curvature effects become relevant. Thus, if the Fermi surface is regular and curved, and if the coupling constant is chosen sufficiently small, *depending on the Fermi surface and thus in particular on the electron density*, the instability will always be of a superconducting type.

However, if the initial coupling constant is held fixed as the density varies, it may, even though small, be so large that the one-loop flow leaves the weak-coupling regime before the curvature effects set in. In this case, a different instability, such as one toward antiferromagnetism, may be stronger than the superconducting instability. The details depend on the parameter regime of the model. (See Refs. 9), 5) and 4) for results from one-loop RG flows.) It should be noted that when the curvature of the Fermi surface is very small, such as when t'/t is small and the filling is near half-filling, the higher-order terms generated by the 1PI six-point function are not suppressed by scaling factors, and therefore these higher-order terms should be taken into account.

1.2.3. The temperature range for Landau Fermi liquid theory

In view of the generic flow to strong coupling, one may ask in what sense one can regard Landau Fermi liquid theory as a "fixed point" of the RG. Because of the Kohn-Luttinger effect, the answer is that (unless time-reversal symmetry is broken explicitly in the free system[15)]) the only true weak-coupling fixed point for $d \geq 2$ is the free fermion point (coupling equal to zero), and it is unstable with respect to any weak four-fermion perturbation, be it attractive or repulsive. The true meaning of the Landau Fermi liquid "fixed point" in this context is that, although the flow eventually leads away from the zero-coupling fixed point, it may remain in its vicinity for a very long flow time, i.e., to very low energy scales. Since temperature

sets a natural energy scale at which the renormalization group flow stops, it poses a natural restriction on the maximal flow time. Thus, if the temperature is high enough, more precisely if $|g_0| \log \beta\epsilon_0 \ll 1$, the system always remains weakly coupled, and Landau Fermi liquid theory can be justified by convergent renormalized perturbation theory.[2),3),17)] As discussed in Refs. 2) and 3), this is also the physically natural definition of Fermi liquid theory: Fermi liquids can be observed only above a critical temperature where superconductivity or some other kind of symmetry breaking sets in. (This temperature may be very low.) Above this temperature, the k-space occupation number density does not have a discontinuity, but the Fermi surface can be identified simply by the scaling of the maximal slope in the occupation density as a function of temperature. For a Fermi liquid, the derivative of the occupation number density becomes of order β at the Fermi surface, as in the Fermi gas, where the occupation number is simply $(1 + e^{\beta e(p)})^{-1}$, and only the prefactor changes due to a finite wave function renormalization. For a Luttinger liquid, the anomalous scaling of the two-point function (corresponding to an infinite wave function renormalization), leads to a scaling with β^α, $\alpha < 1$. If a gap occurs, the slope no longer scales with the temperature. This criterion also corresponds to what is done in experiments — the integrated intensity measured in photoemission experiments allows reconstruction of the occupation density if the interaction matrix elements are known.[19)] Theoretically, verifying that the slope of the occupation number density scales as in the Fermi gas corresponds to showing that the first two derivatives of the self-energy are finite. This was first done in Refs. 2) and 12). Moreover, if $|g_0| \log \beta\epsilon_0 \ll 1$, the Cooper instability does not lead to large coupling constants, and therefore the Landau function describing the interaction of the quasiparticles is well-defined.

1.2.4. Larger initial coupling constants

While the above discussion is largely about initially weakly coupled systems, it may happen that regime 2, where the couplings are not small but the restricted phase space justifies one-loop flows, still exists. If the exact integration over modes with energies above ϵ_1 leaves a system with a curved Fermi surface, and if that curvature is large enough that the corrections to the nonoverlapping part of the flow are small, then one can still use the one-loop approximation to do reliable calculations in regime 2, and thus justify Fermi liquid theory above the critical temperature of the superconducting transition. That this condition is ever fulfilled is not at all obvious, but it seems possible.

§2. The renormalization group

In this section, we present the renormalization group (RG) setup and then discuss its application to our problem. We first review the path integral representation very briefly; the RG is introduced as a transformation that leaves the generating function for the correlation functions invariant.

2.1. *The path integral representation*

We consider a fermionic system with creation and annihilation operators $a^+_{\boldsymbol{x},\sigma}$ and $a_{\boldsymbol{x},\sigma}$ (here σ is $+$ or $-$, which represents the spin in units $\hbar/2$), which obey the canonical anticommutation relations, and with a Hamiltonian $H(a^+, a)$ that is a polynomial in the fermion operators. For instance, a Hubbard-type Hamiltonian is

$$H = \sum_{\boldsymbol{x},\boldsymbol{x}',\sigma} T_{\boldsymbol{x}\boldsymbol{x}'} a^+_{\boldsymbol{x},\sigma} a_{\boldsymbol{x}',\sigma} + \sum_{\boldsymbol{x},\boldsymbol{x}'} : n_{\boldsymbol{x}} V(\boldsymbol{x},\boldsymbol{x}') n_{\boldsymbol{x}'} :, \tag{2}$$

where the number operators $n_{\boldsymbol{x}} = a^+_{\boldsymbol{x},+} a_{\boldsymbol{x},+} + a^+_{\boldsymbol{x},-} a_{\boldsymbol{x},-}$ and the dots denote normal ordering. The Hamiltonian is hermitian if $T_{\boldsymbol{x}\boldsymbol{y}} = \overline{T}_{\boldsymbol{y}\boldsymbol{x}}$ and if $V(\boldsymbol{x},\boldsymbol{x}') = V(\boldsymbol{x}',\boldsymbol{x})$. For a translation-invariant system, $T_{\boldsymbol{x}\boldsymbol{y}} = T(\boldsymbol{x}-\boldsymbol{y})$ and $V(\boldsymbol{x},\boldsymbol{y}) = v(\boldsymbol{x}-\boldsymbol{y})$. The usual repulsive on-site Hubbard interaction is given by $v(\boldsymbol{x}-\boldsymbol{y}) = \frac{U}{2}\delta_{\boldsymbol{x},\boldsymbol{y}}$ with $U > 0$.

The grand canonical trace $Z = \operatorname{Tr} e^{-\beta(H-\mu N)}$ has a representation as a Grassmann functional integral

$$Z = \int \prod_{\tau,\boldsymbol{x},\sigma} d\bar{\psi}_\sigma(\tau,\boldsymbol{x})\, d\psi_\sigma(\tau,\boldsymbol{x}) e^{-\mathcal{A}(\bar{\psi},\psi)}, \tag{3}$$

where the Grassmann fields $\bar{\psi}$ and ψ now depend on an additional Euclidian time τ (which we choose in the interval $-\beta/2 \le \tau < \beta/2$) in which they are antiperiodic. That is, ψ and $\bar{\psi}$ are really defined for all $-\beta \le \tau < \beta$, they are invariant under $\tau \to \tau + 2\beta$, and they satisfy

$$\begin{aligned} \psi_\sigma(\tau+\beta,\boldsymbol{x}) &= -\psi_\sigma(\tau,\boldsymbol{x}), \\ \bar{\psi}_\sigma(\tau+\beta,\boldsymbol{x}) &= -\bar{\psi}_\sigma(\tau,\boldsymbol{x}). \end{aligned} \tag{4}$$

The exponent $\mathcal{A}$ in (3) is the action corresponding to H:

$$\mathcal{A}(\bar{\psi},\psi) = \int_{-\beta/2}^{\beta/2} d\tau \Big[\sum_{\boldsymbol{x},\sigma} \bar{\psi}_\sigma(\tau,\boldsymbol{x})\, \partial_\tau \psi_\sigma(\tau,\boldsymbol{x}) - H\Big(\bar{\psi}(\tau),\psi(\tau)\Big)\Big]. \tag{5}$$

The first summand is the analogue of the usual $p\dot{q}$ term in the Legendre transform. The second is just the Hamiltonian itself, in normal ordered form, and with $a^+_{\sigma,\boldsymbol{x}}$ replaced by $\bar{\psi}_\sigma(\tau,\boldsymbol{x})$ and $a_{\sigma,\boldsymbol{x}}$ replaced by $\psi_\sigma(\tau,\boldsymbol{x})$.

Strictly speaking, the functional integral is the limit $n \to \infty$ of a finite-dimensional Grassmann integral with discrete times $\tau_k = -\beta + \frac{k}{n}\beta$, $0 \le k < n$. At finite n, the analogue of the functional integral (3) is just a finite-dimensional Grassmann integral. Taking the limit $n \to \infty$ is a standard procedure (see, e.g. Refs. 1) and 3)).

For the Hamiltonian (2), the action consists of a quadratic and a quartic term in the fields: $\mathcal{A} = \mathcal{A}_2 + \mathcal{A}_4$. The quadratic term is

$$\mathcal{A}_2(\bar{\psi},\psi) = (\bar{\psi},\, Q\psi), \tag{6}$$

where, for Grassmann fields ψ and $\bar{\eta}$, we have defined the fermionic bilinear form

$$(\bar{\eta},\, \psi) = \int d\xi\, \bar{\eta}(\xi)\, \psi(\xi), \tag{7}$$

used the integral notation $\int d\xi\, F(\xi) = \int_{-\beta/2}^{\beta/2} d\tau \sum_{\boldsymbol{x},\sigma} F(\tau, \boldsymbol{x}, \sigma)$ (with $\xi = (\tau, \boldsymbol{x}, \sigma)$), and denoted the quadratic operator in the action by Q:

$$Q(\xi, \xi') = \delta_{\sigma\sigma'}\delta(\tau - \tau')\Big(\delta_{\boldsymbol{x}\boldsymbol{x}'}(\partial_\tau + \mu) - T_{\boldsymbol{x}\boldsymbol{x}'}\Big). \tag{8}$$

The bilinear form satisfies $(\bar\eta,\, \psi) = -(\psi, \bar\eta)$ because the Grassmann fields anticommute. The quartic term is

$$\mathcal{A}_4(\bar\psi, \psi) = \int_{-\beta/2}^{\beta/2} d\tau \sum_{\boldsymbol{x},\boldsymbol{x}',\sigma,\sigma'} \bar\psi_\sigma(\tau, \boldsymbol{x})\psi_\sigma(\tau, \boldsymbol{x})V(\boldsymbol{x}, \boldsymbol{x}')\bar\psi_{\sigma'}(\tau, \boldsymbol{x}')\psi_{\sigma'}(\tau, \boldsymbol{x}'). \tag{9}$$

The action has all the symmetries of the Hamiltonian. Moreover, the action and the integration measure, and hence the partition function, are invariant under the transformation

$$\psi_\sigma(\tau, \boldsymbol{x}) \to i\bar\psi_\sigma(-\tau, \boldsymbol{x}), \quad \bar\psi_\sigma(\tau, \boldsymbol{x}) \to i\psi_\sigma(-\tau, \boldsymbol{x}). \tag{10}$$

Observables transform accordingly (similarly to the case when taking adjoints).

It is convenient, and natural, to combine the exponential of the quadratic part of the action and the Grassmann product measure into a Grassmann Gaussian measure

$$d\mu_C(\bar\psi, \psi) = \frac{1}{\det Q} \prod_\xi d\bar\psi(\xi)\, d\psi(\xi)\; e^{-\mathcal{A}_2(\bar\psi,\psi)}. \tag{11}$$

The covariance C is the inverse, $C = Q^{-1}$. The inverse exists because the boundary conditions are antiperiodic. We also write $\mathcal{A}_4(\bar\psi, \psi) = \mathcal{V}(\bar\psi, \psi)$.

For a translation-invariant system, C can be calculated as the Fourier transform

$$C(\xi; \xi') = \frac{\delta_{\sigma\sigma'}}{\beta L^d} \sum_\omega \sum_{\boldsymbol{p}} e^{i(\tau-\tau')\omega + i(\boldsymbol{x}-\boldsymbol{x}')\boldsymbol{p}}\, \hat C(\omega, \boldsymbol{p}), \tag{12}$$

of $\hat C(\omega, \boldsymbol{p}) = (i\omega - e(\boldsymbol{p}))^{-1}$, with $e(\boldsymbol{p}) = \hat T(\boldsymbol{p}) - \mu$, where $\hat T$ denotes the Fourier transform of the hopping amplitude T. The summation over $\boldsymbol{p}$ is over the reciprocal lattice, and the sum over ω runs over all Matsubara frequencies, $\omega_n = \frac{\pi}{\beta}(2n + 1)$, where n is an integer. Thus $\hat C$ is simply the usual Matsubara propagator. The value of C at coinciding times is defined as the limit $\tau' \uparrow \tau$, as required by time ordering.

With these definitions, and with Grassmann source terms η and $\bar\eta$, the generating function for the connected Green functions is

$$W(\bar\eta, \eta) = -\log \int d\mu_C(\bar\psi, \psi) e^{-\mathcal{V}(\bar\psi,\psi) + (\bar\eta,\psi) + (\bar\psi,\eta)}. \tag{13}$$

The quantity Z in (3) is now $e^{-W(0,0)} \det Q$. All information about the system is contained in the connected correlation functions, which are the derivatives of $\log Z(\bar\eta, \eta)$ with respect to the source terms $\bar\eta$ and η, at $\eta = \bar\eta = 0$. When $\mathcal{V} = 0$, the fermions are noninteracting, the integral for Z is Gaussian, and $W(\bar\eta, \eta) = -(\bar\eta, C\eta)$. This implies that the correlation functions are determinants of the two-point function (or covariance) C.

Thus all objects appearing in the functional integral have a natural interpretation. The Gaussian measure with covariance C describes free fields, i.e. particles with propagator C. The interaction appears in the form of an (unnormalized) Boltzmann factor $e^{-\mathcal{V}}$. Thus our system is characterized by C and $\mathcal{V}$. The renormalization group is a transformation of C and $\mathcal{V}$ which depends on an energy scale and which leaves $Z(\bar{\eta}, \eta)$ invariant.

Performing a shift in the integration variables, we obtain

$$e^{-W(\bar{\eta},\eta)} = e^{(\bar{\eta},C\eta)} \int d\mu_C(\bar{\psi},\psi) e^{-\mathcal{V}(\bar{\psi}-C^T\bar{\eta},\,\psi-C\eta)}. \tag{14}$$

Here C^T is the transpose of C. The function

$$\mathcal{G}(\bar{\phi},\phi) = -\log \int d\mu_C(\bar{\psi},\psi) e^{-\mathcal{V}(\bar{\psi}+\bar{\phi},\,\psi+\phi)} \tag{15}$$

is called the effective action. We have $W(\bar{\eta},\eta) = (\bar{\eta}, C\eta) - \mathcal{G}(C^T\bar{\eta}, C\eta)$, so studying W is equivalent to studying $\mathcal{G}$.

We now streamline the notation and introduce Nambu-type fields, to make the derivation of the RG equations simpler. Let $X = (\tau, \boldsymbol{x}, \sigma, c)$, where the charge index $c = \pm 1$ distinguishes between ψ and $\bar{\psi}$. With the Grassmann field $\Psi(X)$ given by

$$\Psi(\tau,\boldsymbol{x},\sigma,1) = \bar{\psi}_\sigma(\tau,\boldsymbol{x}), \qquad \Psi(\tau,\boldsymbol{x},\sigma,-1) = \psi_\sigma(\tau,\boldsymbol{x}), \tag{16}$$

the quadratic part of the action is

$$(\bar{\psi}, Q\psi) = \frac{1}{2}\left((\bar{\psi},\psi), \begin{pmatrix} 0 & Q \\ -Q^T & 0 \end{pmatrix} \begin{pmatrix} \bar{\psi} \\ \psi \end{pmatrix}\right) = \frac{1}{2}(\Psi, \boldsymbol{Q}\,\Psi), \tag{17}$$

with $Q^T(\xi,\xi') = Q(\xi',\xi)$. Thus $\boldsymbol{Q}$ satisfies $\boldsymbol{Q}^T = -\boldsymbol{Q}$. Because the source terms are

$$(\bar{\eta},\psi) + (\bar{\psi},\eta) = (H,\Psi), \quad \text{with } H = \begin{pmatrix} -\eta \\ \bar{\eta} \end{pmatrix}, \tag{18}$$

we have (with $\boldsymbol{C} = \boldsymbol{Q}^{-1}$)

$$\int d\mu_C(\bar{\psi},\psi) e^{(\bar{\eta},\psi)+(\bar{\psi},\eta)} = \int d\mu_{\boldsymbol{C}}(\Psi) e^{(H,\Psi)} = e^{-\frac{1}{2}(H,\boldsymbol{C}H)}. \tag{19}$$

The exponential of the effective action $\mathcal{G}$ is the convolution

$$e^{\mathcal{G}(\boldsymbol{C},\mathcal{V})(\Phi)} = \int d\mu_{\boldsymbol{C}}(\Psi) e^{-\mathcal{V}(\Psi+\Phi)} = \left(\mu_{\boldsymbol{C}} * e^{\mathcal{V}}\right)(\Phi). \tag{20}$$

We do not require $\boldsymbol{Q}$ to be of the form in (17), but only that it be antisymmetric. Thus it may have diagonal terms, which correspond to non-charge invariant terms, such as a superconducting gap.

2.2. *RG flow: general setup*

The semigroup law of the RG is based on the addition principle for Gaussian fields: If $\boldsymbol{C} = \boldsymbol{C}_1 + \boldsymbol{C}_2$, then Ψ splits into two independent fields, as $\Psi = \Psi_1 + \Psi_2$, where Ψ_1 has covariance $\boldsymbol{C}_1$ and Ψ_2 has covariance $\boldsymbol{C}_2$. The corresponding Gaussian measure factorizes, so that

$$\int d\mu_{\boldsymbol{C}}(\Psi) e^{-\mathcal{V}(\Psi+\Phi)} = \int d\mu_{\boldsymbol{C}_1}(\Psi_1) \int d\mu_{\boldsymbol{C}_2}(\Psi_2) e^{-\mathcal{V}(\Psi_1+\Psi_2+\Phi)}. \tag{21}$$

When one starts out at weak coupling, it is natural to label energy scales according to the kinetic energy. In the following, we use the decomposition $\boldsymbol{C} = \boldsymbol{D}_s + \boldsymbol{C}_s$ with a scale parameter $s \geq 0$ corresponding to an energy scale $\epsilon_s = \epsilon_0 e^{-s}$. The propagator $\boldsymbol{C}_s$ corresponds to fields with energy $e(\boldsymbol{p})$ above ϵ_s, and $\boldsymbol{D}_s$ to fields with energy below ϵ_s. The effective action in which the fields with propagator $\boldsymbol{C}_s$ have been integrated out is $\mathcal{G}_{\epsilon_s} = \mathcal{G}(\boldsymbol{C}_s, \mathcal{V})$. In the limit $s \to \infty$, where the energy scale ϵ_s vanishes, $\boldsymbol{D}_s$ is identically zero and everything has been integrated out. Inserting this decomposition and using (21), we get for the effective action $\mathcal{G}_0 = \mathcal{G}(\boldsymbol{C}, \mathcal{V})$, in which all fields have been integrated over,

$$\begin{aligned} e^{-\mathcal{G}_0(\Phi)} &= \int d\mu_{\boldsymbol{D}_s+\boldsymbol{C}_s}(\Psi) e^{-\mathcal{V}(\Psi+\Phi)} \\ &= \int d\mu_{\boldsymbol{D}_s}(\Psi') e^{-\mathcal{G}_{\epsilon_s}(\Psi'+\Phi)}. \end{aligned} \tag{22}$$

Equation (22) is the semigroup law of the RG. It can also be written in the form

$$\mathcal{G}(\boldsymbol{D}_s + \boldsymbol{C}_s, \mathcal{V}) = \mathcal{G}(\boldsymbol{D}_s, \mathcal{G}(\boldsymbol{C}_s, \mathcal{V})). \tag{23}$$

The semigroup law implies that the system $(\boldsymbol{C}, \mathcal{V})$ that we wish to study is exactly equivalent to the system $(\boldsymbol{D}_s, \mathcal{G}(\boldsymbol{C}_s, \mathcal{V}))$ with propagator $\boldsymbol{D}_s$ and effective interaction $\mathcal{G}(\boldsymbol{C}_s, \mathcal{V})$. It also shows that the effective action $\mathcal{G}(\boldsymbol{C}_s, \mathcal{V})$ generates the connected, amputated correlation functions of the model with covariance $\boldsymbol{C}_s$. In our application, $\boldsymbol{C}_s$ is a covariance with infrared cutoff ϵ_s, and $\boldsymbol{D}_s$ is supported on a smaller momentum space, because it is nonzero only for fields with energies smaller than ϵ_s.

Set up in this way, the renormalization group is simply a symmetry of the generating functional $\mathcal{G}(\boldsymbol{C}, \mathcal{V})$, which contains all the information for the model. The RG differential equation expresses this statement in differential form, namely that $\mathcal{G}(\boldsymbol{C}, \mathcal{V})$ is independent of s. Thus the RGDE is the equation $\frac{\partial}{\partial s}\mathcal{G}(\boldsymbol{C}, \mathcal{V}) = 0$, evaluated by inserting the right-hand side of (22).

The exact symmetry comes at a price: $\mathcal{G}$ is a more complicated function than the original interaction. It is an infinite power series of the form

$$\begin{aligned} \mathcal{G}_{\epsilon_s}(\psi) = \sum_{\sigma} \int dp\, \bar{\psi}_\sigma(p) \hat{B}_{\epsilon_s}(p) \psi_\sigma(p) + \sum_{\sigma_1,\cdots,\sigma_4} \int dp_1 \cdots dp_4 \\ \{\bar{\psi}_{\sigma_1}(p_1)\bar{\psi}_{\sigma_2}(p_2)\psi_{\sigma_3}(p_3)\psi_{\sigma_4}(p_4)\delta(p_1+p_2-p_3-p_4)\hat{F}^{(\epsilon_s)}_{\sigma_1,\cdots,\sigma_4}(p_1,p_2,p_3)\} \\ + \text{ terms of order } \psi^6, \quad \psi^8, \cdots \end{aligned} \tag{24}$$

in the fields. We are mainly concerned with the quadratic and quartic terms, which have the significance of the self-energy correction and the effective interaction. However, one should be aware that the interactions corresponding to the terms of order ψ^6 or higher are always present and that the convergence of the infinite series is a nontrivial problem. (It is shown to converge in two dimensions in Ref. 13).) The self-energy term B produces, among other things, a Fermi surface shift, which has to be kept track of in the flow. This has been done for general Fermi surfaces. [11)]

In the following, we derive a differential equation for the one-particle-irreducible (1PI) functions, from which we can obtain the above functions B and F. This derivation is similar to that used in Ref. 2), except that we do not use Wick ordering here and give the equations for the 1PI functions. The Wick-ordered equation of Ref. 2) is used in Ref. 5). Yet another form (the original one of Polchinski) is used in Ref. 4). In an exact treatment, all these approaches are equivalent, because they give the same correlation functions. In approximations obtained by truncations of the equations, the question of equivalence becomes nontrivial. From the technical point of view, there are a number of differences, on which we comment below.

To summarize, the RG expresses the generating function of our field theory in the form

$$\int d\mu_{\boldsymbol{C}}(\Psi) e^{-\mathcal{V}(\Psi+\Phi)} = \int d\mu_{\tilde{\boldsymbol{D}}_s}(\Psi) e^{-\tilde{\mathcal{V}}_s(\Psi+\Phi)} \,. \tag{25}$$

In the way derived above, we have $\tilde{\boldsymbol{D}}_s = \boldsymbol{D}_s$ and $\tilde{\mathcal{V}}_s = \mathcal{G}(\boldsymbol{C}_s, \mathcal{V})$, but other choices are possible. In general, $\mathcal{G}(\boldsymbol{C}_s, \mathcal{V})$ will contain a self-energy term (quadratic in the fields), which we absorb in the new propagator $\tilde{\boldsymbol{D}}_s$ later to deal with the flow of the Fermi surface and the superconducting gap.

Note that because the generating function is invariant under the decomposition, we are able to stop the flow at any scale we want. This will be necessary because our flows generically lead to strong coupling.

§3. The RG for the 1PI functions

In the following, we derive the RG for the 1PI functions. For the moment, we do not need all the details of the setup in terms of scale parameters. We only use the fact that $\boldsymbol{C}_s$ depends on the parameter s. Recall that studying W (given in (13)) is equivalent to studying $\mathcal{G}$. The 1PI functions are generated by the first Legendre transform Γ of W.

3.1. *The generating function of the 1PI vertices*

In a general theory with fermionic fields, the fields $\psi(X)$ and $\bar{\psi}(X)$ are labelled by an index X, which comprises spacetime, spin, flavour, and other possible indices. We collect ψ and $\bar{\psi}$ into a single vector $\Psi = (\bar{\psi}, \psi)$. We also use the notation $(A, B) = \int dX A(X) B(X)$, where $\int dX$ stands for summation over the discrete indices and integrals over the continuous indices. In the Hubbard model, the standard functional integral representation (see, e.g. Ref. 3), §4.2) gives $X = (\tau, \boldsymbol{x}, \sigma, c)$, where $\boldsymbol{x}$ is the position, $\sigma = \pm$ the third component of the spin, τ (satisfying $-\beta/2 \leq \tau < \beta/2$) is the usual Euclidian time used to convert the grand canonical trace into a functional

integral over the Grassmann fields Ψ, and where the charge index $c = \pm$ distinguishes between the components ψ and $\bar{\psi}$ of Ψ.

The generating function for the connected non-amputated Green functions is defined by

$$e^{-W(H)} = \int d\mu_{\boldsymbol{C}}(\Psi) e^{-\mathcal{V}(\Psi)+(H,\Psi)} \,. \tag{26}$$

Here the Gaussian integral is given by an invertible operator $\boldsymbol{Q}$ with integral kernel $\boldsymbol{Q}(X, X')$. Because of the Grassmann nature of the fields, $\boldsymbol{Q}$ is antisymmetric, i.e. $\boldsymbol{Q}(X', X) = -\boldsymbol{Q}(X, X')$. The covariance $\boldsymbol{C}$ is $\boldsymbol{C} = \boldsymbol{Q}^{-1}$, and $d\mu_{\boldsymbol{C}}(\Psi) = (\det \boldsymbol{Q})^{-1} e^{-\frac{1}{2}(\Psi, \boldsymbol{Q}\Psi)} D\bar{\psi} D\psi$, with the notation (A, B) as defined above. A general antisymmetric $\boldsymbol{Q}$ includes from the start the possibility of non-charge invariant terms of type $\psi(X)\psi(X')$; charge invariance corresponds to a matrix $\boldsymbol{Q}$ of the form

$$\big(\boldsymbol{Q}(\xi, \xi')\big)_{cc'} = \begin{pmatrix} 0 & Q(\xi, \xi') \\ -Q(\xi', \xi) & 0 \end{pmatrix} . \tag{27}$$

In the Hubbard model,

$$Q(\xi, \xi') = \delta_{\sigma\sigma'} \delta(\tau - \tau') \Big(\delta_{\boldsymbol{x}\boldsymbol{x}'} (\partial_\tau + \mu) - T_{\boldsymbol{x}\boldsymbol{x}'} \Big), \tag{28}$$

where T denotes the hopping matrix. $\mathcal{V}$ is the interaction term written in terms of the fields Ψ (for details, see e.g. Ref. 3)).

The source term H is another Grassmann vector. If $H = \binom{-\eta}{\bar{\eta}}$, then (H, Ψ) is the usual combination $(\bar{\eta}, \psi) + (\bar{\psi}, \eta)$. If W has a nondegenerate quadratic part, the map $H \mapsto \Phi_{cl}(H)$, with

$$\Phi_{cl}(H)(X) = \frac{\delta}{\delta H(X)} W(H), \tag{29}$$

can be inverted. (This is the case in our fermionic models because the Grassmann variables are nilpotent and the covariance $\boldsymbol{C}$ is nondegenerate at positive temperature. In bosonic models, the map would not be invertible if symmetry breaking occurs. In this case the Legendre transform is then defined by a variational equation, as discussed, e.g. in Ref. 7)). We denote the inverse map by $\phi \mapsto h(\phi)$ (when h is an odd element of the Grassmann algebra generated by ϕ), so that

$$\Phi_{cl}\Big(h(\phi)\Big) = \frac{\delta W}{\delta H}\Big(h(\phi)\Big) = \phi \,. \tag{30}$$

Taking the derivative with respect to ϕ gives

$$\int dZ \frac{\delta h(\phi)(Z)}{\delta \phi(Y)} \left(\frac{\delta^2 W}{\delta H(Z) \delta H(X)} \right) (h(\phi)) = \delta(X, Y) \,. \tag{31}$$

The first Legendre transform of W is

$$\Gamma(\phi) = W\left(h(\phi)\right) - \left(h(\phi), \phi\right), \tag{32}$$

with the last term a bilinear form as above. This generates the 1PI correlation functions. We have $\frac{\delta \Gamma}{\delta \phi} = h(\phi)$, and thus by (31) (as operators)

$$\left(\frac{\delta^2 \Gamma}{\delta \phi^2}\right)(\phi) = \left[\frac{\delta^2 W}{\delta H^2}\Big(h(\phi)\Big)\right]^{-1}. \tag{33}$$

For free particles ($\mathcal{V} = 0$), $W = \frac{1}{2}(H, \boldsymbol{C}H)$, so $\delta W/\delta H = \boldsymbol{C}H$, and hence $h(\phi) = \boldsymbol{C}^{-1}\phi$, and $\Gamma(\phi) = \frac{1}{2}(\phi, \boldsymbol{C}^{-1}\phi)$. At first order, the four-fermion interaction term in Γ is just the original interaction $\mathcal{V}$.

3.2. *The RG differential equation for Γ*

If W depends on the parameter s, then Γ and h also depend on s. By (30), we have

$$\frac{d}{ds} W_s(h_s(\phi)) = \frac{\partial W_s}{\partial s}(h_s(\phi)) + (\dot{h}_s(\phi), \phi), \tag{34}$$

where the dot denotes differentiation with respect to s. Thus (32) implies

$$\dot{\Gamma}_s(\phi) = \dot{W}_s\Big(h_s(\phi)\Big). \tag{35}$$

We now assume that the s-dependence of W_s is given as follows. In (26), $\mathcal{V}$ remains independent of s, but $\boldsymbol{C}$ is replaced by $\boldsymbol{C}_s = \boldsymbol{Q}_s^{-1}$, where $\boldsymbol{Q}_s$ now depends on s. Then the derivative $\partial/\partial s$ can act only on $d\mu_{\boldsymbol{C}_s}$, that is, on the normalization factor or on the exponent. In the former case, it just produces a constant term, and in the latter case it brings $(\Psi, \dot{\boldsymbol{Q}}_s \Psi)$ into the integral. Using

$$(\Psi, \dot{\boldsymbol{Q}}_s \Psi)\, e^{(H,\Psi)} = \left(\frac{\delta}{\delta H}, \dot{\boldsymbol{Q}}_s \frac{\delta}{\delta H}\right)\, e^{(H,\Psi)}, \tag{36}$$

we can reexpress everything in terms of $W_s(H)$ and get

$$\dot{W}_s(H) = \frac{1}{2}\, \mathrm{Tr}\,(\boldsymbol{C}_s \dot{\boldsymbol{Q}}_s) + \frac{1}{2}\left(\frac{\delta}{\delta H}, \dot{\boldsymbol{Q}}_s \frac{\delta}{\delta H}\right) W_s(H) + \frac{1}{2}\left(\frac{\delta W_s}{\delta H}, \dot{\boldsymbol{Q}}_s \frac{\delta W_s}{\delta H}\right) \tag{37}$$

and $\mathrm{Tr}\,(AB) = \int dX\, dY\, A(X,Y)B(Y,X)$. This is similar to Polchinski's equation,[6] but with $\boldsymbol{Q}_s$ replacing $\boldsymbol{C}_s$ in the Laplacian, because the Green functions generated by W are not amputated. From (35), (30) and (33), the differential equation for $\Gamma(s)$ is found to be

$$\dot{\Gamma}(s|\phi) = \frac{1}{2}\, \mathrm{Tr}\,(\boldsymbol{C}_s \dot{\boldsymbol{Q}}_s) + \frac{1}{2}(\phi, \dot{\boldsymbol{Q}}_s \phi) + \frac{1}{2}\, \mathrm{Tr}\, \left[\dot{\boldsymbol{Q}}_s \left(\frac{\delta^2 \Gamma(s|\phi)}{\delta \phi^2}\right)^{-1}\right]. \tag{38}$$

This is a nonpolynomial equation for Γ, but the inverse contains a second derivative, which produces a field-independent term coming from the quadratic term in Γ. Thus the equation makes sense in an expansion in the fields.

3.3. *Expansion in the fields*

In this section we derive the equation for the scale-dependent 1PI m-point functions $\gamma_m(s)$, by expanding $\Gamma(s|\phi)$ in the fields. Readers that only wish to see the result can skip to the next subsection.

The 1PI m-point vertex functions $\gamma_m(s|X_1, \cdots, X_m)$ are the coefficients in the expansion of Γ as a power series in the fields:

$$\Gamma(s|\phi) = \sum_{m\geq 0} \gamma^{(m)}(s|\phi) \tag{39}$$

with

$$\gamma^{(m)}(s|\phi) = \frac{1}{m!} \int d^m \underline{X}\, \gamma_m(s|\underline{X})\, \phi^m(\underline{X})\,. \tag{40}$$

Here we used the definitions $\underline{X} = (X_1, \cdots, X_m)$ and $\phi^m(\underline{X}) = \phi(X_1)\cdots\phi(X_m)$. We choose the function $\gamma_m(s|\underline{X})$ to be totally antisymmetric: $\mathcal{A}_m\gamma_m = \gamma_m$, where $(\mathcal{A}_m F)(X_1, \cdots, X_m) = \frac{1}{m!}\sum_\pi \epsilon(\pi) F(X_{\pi(1)}, \cdots, X_{\pi(m)})$ is the antisymmetrization operator. (π is summed over all permutations of $1, \cdots, m$, and $\epsilon(\pi)$ denotes the sign of π.) Any part of γ_m that is not antisymmetric would cancel out in (40), because of the antisymmetry properties of the Grassmann variables. Also, below we compare coefficients. This is allowed only when totally antisymmetric functions are used. The $\gamma_m(s|\underline{X})$ are the 1PI vertex functions. Similarly, we have the expansion

$$\frac{\delta}{\delta\phi(X)}\frac{\delta}{\delta\phi(Y)}\Gamma(s|\phi) = \sum_{m\geq 0} \tilde{\gamma}^{(m)}(s|X, Y; \phi)\,. \tag{41}$$

By the antisymmetry of γ_m, two derivatives applied to $\gamma^{(m+2)}$ give the factor $(m+2)(m+1)$, which combines with the $1/(m+2)!$ to yield $1/m!$. (This is the reason for the convention of putting the prefactor $\frac{1}{m!}$ in (40).) Thus

$$\tilde{\gamma}^{(m)}(s|X, Y; \phi) = \frac{1}{m!} \int d^m \underline{X}'\gamma_{m+2}(s|X, Y, \underline{X}')\phi^m(\underline{X}')\,. \tag{42}$$

In particular, $\tilde{\gamma}^{(0)}$ is independent of ϕ:

$$\tilde{\gamma}^{(0)}(s|X, Y; \phi) = \gamma_2(s|X, Y)\,. \tag{43}$$

Therefore

$$\frac{\delta^2\Gamma(s|\phi)}{\delta\phi(X)\delta\phi(Y)} = \gamma_2(s|X, Y) + \tilde{\Gamma}(s|X, Y; \phi), \tag{44}$$

with

$$\tilde{\Gamma}(s|X, Y; \phi) = \sum_{m\geq 2} \tilde{\gamma}^{(m)}(s|X, Y; \phi)\,. \tag{45}$$

It is natural to think of $\gamma_2(s|X, Y)$ and $\tilde{\Gamma}(s|X, Y; \phi)$ as integral kernels of the operators γ_2 and $\tilde{\Gamma}(s|\phi)$. From relation (33) at $\phi = 0$, we find that

$$\boldsymbol{G}_s = \gamma_2(s)^{-1} \tag{46}$$

is the full two-point function. As an equation between operators, we thus have

$$\frac{\delta^2\Gamma}{\delta\phi^2}(s|\phi) = \gamma_2\Big(1 + \boldsymbol{G}_s\tilde{\Gamma}(s|\phi)\Big)\,, \tag{47}$$

and hence the differential equation for Γ now reads

$$\dot{\Gamma}(s|\phi) = \frac{1}{2}\,\mathrm{Tr}\,(\boldsymbol{C}_s\dot{\boldsymbol{Q}}_s) + \frac{1}{2}(\phi, \dot{\boldsymbol{Q}}_s\phi) + \frac{1}{2}\,\mathrm{Tr}\,\Big[\boldsymbol{G}_s\dot{\boldsymbol{Q}}_s\Big(1 + \boldsymbol{G}_s\tilde{\Gamma}(s|\phi)\Big)^{-1}\Big]\,. \tag{48}$$

This equation is a nonpolynomial in Γ because of the irreducibility condition. We get the equations for the γ_m by expanding $\Big(1 + \boldsymbol{G}_s\tilde{\Gamma}(s|\phi)\Big)^{-1}$ in a geometric series:

$$\begin{aligned}&\mathrm{Tr}\,\Big[\boldsymbol{G}_s\dot{\boldsymbol{Q}}_s\Big(1 + \boldsymbol{G}_s\tilde{\Gamma}(s\mid\phi)\Big)^{-1}\Big]\\ &= \mathrm{Tr}\,(\boldsymbol{G}_s\dot{\boldsymbol{Q}}_s) - \mathrm{Tr}\,\Big(\boldsymbol{G}_s\dot{\boldsymbol{Q}}_s\boldsymbol{G}_s\tilde{\Gamma}(s|\phi)\Big) + \sum_{p\geq 2}(-1)^p\,\mathrm{Tr}\,\Big[\boldsymbol{G}_s\dot{\boldsymbol{Q}}_s\Big(\boldsymbol{G}_s\tilde{\Gamma}(s|\phi)\Big)^p\Big]\,.\end{aligned} \tag{49}$$

The first term here is a constant, which corresponds to a vacuum energy and is not interesting for our purposes because it drops out in all correlation functions. The term linear in $\tilde{\Gamma}$ generates contractions with single lines. Its lowest order in ϕ is quadratic in ϕ, and therefore it generates self-energy corrections. The graphical interpretation of the terms with $p \geq 2$ is also straightforward: The pth order term $\Big(\boldsymbol{G}_s\tilde{\Gamma}(s|\phi)\Big)^p\boldsymbol{G}_s$ is a linear tree with p vertices. Taking the trace with $\dot{\boldsymbol{Q}}_s$ forms a loop. Thus in the graphical expansion, only 1PI graphs contribute to Γ.

We define the single-scale propagator as

$$\boldsymbol{S}_s = -\boldsymbol{G}_s\dot{\boldsymbol{Q}}_s\boldsymbol{G}_s. \tag{50}$$

The quantities $\tilde{\gamma}^{(m)}$ defined in (42) are homogeneous of degree m in ϕ. Inserting (39) into the left-hand side and (45) into the right-hand side of (48), we get a system of equations for the $\gamma^{(m)}$. For $m \leq 6$ these equations are

$$\dot{\gamma}^{(2)}(s|\phi) = \frac{1}{2}(\phi, \dot{\boldsymbol{Q}}_s\phi) + \frac{1}{2}\,\mathrm{Tr}\,\Big(\boldsymbol{S}_s\tilde{\gamma}^{(2)}(s|\phi)\Big), \tag{51}$$

$$\dot{\gamma}^{(4)}(s|\phi) = \frac{1}{2}\,\mathrm{Tr}\,\Big[\boldsymbol{S}_s\tilde{\gamma}^{(4)}(s\mid\phi)\Big] - \frac{1}{2}\,\mathrm{Tr}\,\Big[\boldsymbol{S}_s\tilde{\gamma}^{(2)}(s\mid\phi)\boldsymbol{G}_s\tilde{\gamma}^{(2)}(s|\phi)\Big], \tag{52}$$

$$\begin{aligned}\dot{\gamma}^{(6)}(s|\phi) = {}&\frac{1}{2}\,\mathrm{Tr}\,\Big[\boldsymbol{S}_s\tilde{\gamma}^{(6)}(s|\phi)\Big]\\ &-\frac{1}{2}\,\mathrm{Tr}\,\Big[\boldsymbol{S}_s(\tilde{\gamma}^{(4)}\boldsymbol{G}_s\tilde{\gamma}^{(2)} + \tilde{\gamma}^{(2)}\boldsymbol{G}_s\tilde{\gamma}^{(4)})\Big] + \frac{1}{2}\,\mathrm{Tr}\,[\boldsymbol{S}_s\tilde{\gamma}^{(2)}\boldsymbol{G}_s\tilde{\gamma}^{(2)}\boldsymbol{G}_s\tilde{\gamma}^{(2)}].\end{aligned} \tag{53}$$

The last term contributing to $\dot{\gamma}^{(4)}$ is

$$\mathrm{Tr}\,(\boldsymbol{S}_s\tilde{\gamma}^{(2)}\boldsymbol{G}_s\tilde{\gamma}^{(2)}) = \int dX_1 \cdots dX_4\,\phi(X_1)\cdots\phi(X_4)\mathcal{T}_4, \tag{54}$$

with

$$\begin{aligned}\mathcal{T}_4 = \int\, & dY_1 \cdots dY_4\;\boldsymbol{S}_s(Y_1, Y_2)\;\boldsymbol{G}_s(Y_3, Y_4)\\ & \frac{1}{2}\gamma_4(s|X_1, X_2, Y_2, Y_3)\;\frac{1}{2}\gamma_4(s|X_3, X_4, Y_4, Y_1)\,.\end{aligned} \tag{55}$$

Thus comparing coefficients of $\phi(X_1)\cdots\phi(X_4)$ gives, with $\underline{X} = (X_1, \cdots, X_4)$,

$$\dot{\gamma}_4(s|\underline{X}) = \frac{1}{2}\int dY_1\, dY_2\, \gamma_6(s|\underline{X}, Y_1, Y_2)\boldsymbol{S}_s(Y_2, Y_1) - \frac{4!}{2}\mathcal{A}_4\mathcal{T}_4(\underline{X}). \tag{56}$$

Note that $\mathcal{T}_4$, as given in (55), is not in antisymmetrized form, so $\mathcal{A}_4\mathcal{T}_4$ appears in (56) because coefficients can only be compared if they are all antisymmetric. To calculate $\mathcal{A}_4\mathcal{T}_4$, we have to antisymmetrize the product $A_{12}B_{34}$, where $A_{kl} = \gamma_4(s|X_k, X_l, Y_1, Y_3)$ and $B_{kl} = \gamma_4(s|X_k, X_l, Y_4, Y_1)$. The antisymmetrization amounts to obtaining

$$P_4(\underline{X}, \underline{Y}) = \frac{1}{4}\sum_{\pi\in\mathcal{S}_4} \epsilon(\pi) A_{\pi(1)\pi(2)} B_{\pi(3)\pi(4)}\,. \tag{57}$$

By definition, $A_{kl} = -A_{lk}$ and $B_{kl} = -B_{lk}$. The extra factor $\frac{1}{4}$ comes from the two factors $\frac{1}{2}$ in (55). We block the sum over π into those for which $\pi(\{1,2\}) = \{a,b\}$ is fixed. This gives $\binom{4}{2} = 6$ terms. All of them are similar, so we discuss the case $a = 1$, $b = 2$. There are four permutations that leave $\{1,2\}$ fixed, namely the identity, the transposition τ_{12} (of 1 and 2), the transposition τ_{34} and combined transposition $\tau_{12}\circ\tau_{34}$. Taking into account the signs, we have

$$\sum_{\pi:\pi(\{1,2\})=\{1,2\}} \epsilon(\pi) A_{\pi(1)\pi(2)} B_{\pi(3)\pi(4)} = (A_{12} - A_{21})(B_{34} - B_{43}) = 4A_{12}B_{34}, \tag{58}$$

by the antisymmetry of A and B. All other cases of $\pi(\{1,2\})$ are similar; there is a global sign obtained by permuting 1 and a and permuting 2 and b, which for $a < b$ is $(-1)^{a+b-1}$. Thus

$$P_4(\underline{X}, \underline{Y}) = A_{12}B_{34} - A_{13}B_{24} + A_{14}B_{23} + A_{23}B_{14} - A_{24}B_{13} + A_{34}B_{12}. \tag{59}$$

Inserting the definitions of A and B and relabelling the integration variables, we can combine the terms containing A_{12} and B_{12}, A_{13} and B_{13}, etc.

3.4. *The RGDE for the 1PI functions: Truncation*

Denoting $\underline{Y} = (Y_1, \cdots, Y_4)$, we have

$$\boldsymbol{L}(\underline{Y}) = \boldsymbol{S}_s(Y_1, Y_2)\boldsymbol{G}_s(Y_3, Y_4) + \boldsymbol{S}_s(Y_3, Y_4)\boldsymbol{G}_s(Y_1, Y_2), \tag{60}$$

with $\boldsymbol{S}_s$ as in (50), $\boldsymbol{G}_s$ as in (46), and

$$\begin{aligned}\boldsymbol{B}_s(\underline{X}, \underline{Y}) = {} & \gamma_4(s|X_1, X_2, Y_2, Y_3)\gamma_4(s \mid Y_4, Y_1, X_3, X_4) \\ & - \gamma_4(s|X_1, X_3, Y_2, Y_3)\gamma_4(s \mid Y_4, Y_1, X_2, X_4) \\ & + \gamma_4(s|X_1, X_4, Y_2, Y_3)\gamma_4(s \mid Y_4, Y_1, X_2, X_3).\end{aligned} \tag{61}$$

The differential equation for the 1PI four-point function γ_4 is

$$\dot{\gamma}_4(s|\underline{X}) = \frac{1}{2}\int dY_1\, dY_2 \gamma_6(s|\underline{X}, Y_1, Y_2)\boldsymbol{S}_s(Y_2, Y_1) - \frac{1}{2}\int d^4\,\underline{Y}\boldsymbol{L}(\underline{Y})\boldsymbol{B}_s(\underline{X}, \underline{Y}). \tag{62}$$

By (42) and (43), the equation for the 1PI two-point function γ_2 becomes

$$\dot{\gamma}_2(s|X_1, X_2) = \dot{\boldsymbol{Q}}_s(X_1, X_2) + \frac{1}{2}\int dX_3\, dX_4\, \boldsymbol{S}_s(X_4, X_3)\,\gamma_4(s|X_1, X_2, X_3, X_4)\,. \tag{63}$$

Equations (62) and (63) are the first two equations in the infinite system of RG equations (labelled by m). Note that they do not form a closed system because γ_6 enters into (62). This behaviour continues to all m: the right-hand side of the equation for $\dot{\gamma}_m$ contains γ_{m+2}.

A method to close the system of equations for the 1PI four-point function γ_4 and the self-energy is to drop the 1PI six-point vertex from (62). This truncation is equivalent to setting all 1PI functions with $m \geq 6$ external legs to zero, so that the connected (non-1PI) m-point functions with $m \geq 6$ are given by tree graphs made of the four-legged vertices and the approximation of the full propagator provided by the solution of the differential equations. The four-point and two-point differential equations are given in terms of one-loop diagrams.

Note, however, that even the untruncated system of differential equations contains only one-loop terms in every equation. This is the case because in the differential formulation, only one differentiated propagator appears in the equation (and there are no tree terms in an equation for 1PI functions). Of course, this does not imply that only one-loop graphs appear in the solution; the full RG produces, after all, the full Green functions. The perturbation expansion is obtained by integrating the differential equation from 0 to s and then iterating the integral equation so obtained until only bare vertices appear. Upon iteration, graphs with an arbitrary number of loops are generated, and if one uses the untruncated equations, all graphs are generated.

The truncated equations amount to a summation of part of the diagrams, but these diagrams also contain two-loop graphs, in particular two-loop graphs corresponding to the self-energy.

The RG strategy does not necessarily aim at taking into account as many graphs as possible but to single out the important ones by their scaling behaviour. We present discussion in §5 answering in which cases and in which energy regimes the scaling behaviour justifies a truncation of the RGDE.

The initial condition for γ_4 is the bare interaction. To renormalize the Fermi surface correctly, one also needs to take into account a Fermi surface counter term (see Refs. 14), 11) and 12)).

§4. Consequences of symmetries

The derivation of Eqs. (62) and (63) does not require any symmetries, so these equations are also valid when symmetries are broken. In our systems, this means that they also hold in the presence of a superconducting gap, magnetic ordering, or translational symmetry breaking. In two dimensions, continuous symmetry breaking is impossible at any positive temperature, because of the Mermin-Wagner theorem. A noninvariance of the effective action leads immediately to long range order, and hence to mean-field type results. In order to compare competing instabilities, we therefore first assume that all continuous symmetries of the action remain unbroken. This leads to further simplifications in the differential equations, which we now discuss.

4.1. *Charge invariance*

Recalling that $X = (\xi, c)$, where ξ consists of space, time, and spin indices, and where $c = \pm$ is the charge index, charge invariance implies that $\boldsymbol{S}_s((\xi, c), (\xi', c'))$ and $\boldsymbol{G}_s((\xi, c), (\xi', c'))$ are nonzero only if $c \neq c'$, and that $\gamma_4(s|X_1, \cdots, X_4) \neq 0$ only if two of the charge indices are $+$ and two are $-$. Because γ_4 is antisymmetric in all arguments, it is then determined by $f(s|\xi_1, \cdots, \xi_4) = \gamma_4(s|(\xi_1, +), (\xi_2, +), (\xi_3, -), (\xi_4, -))$. Also, f inherits the antisymmetry under exchange of ξ_1 and ξ_2 and that under exchange of ξ_3 and ξ_4.

We now rewrite (62) as an equation for f. The only thing we need to do is to arrange the internal charge index sums. For instance, the first term on the right-hand side of (62) becomes

$$\sum_{c_1,\cdots,c_4} \int d\eta_1 \cdots d\eta_4 \, \boldsymbol{L}((\eta_1, c_1), \cdots, (\eta_4, c_4)) \gamma_4(s \mid (\xi_1, +), (\xi_2, +), (\eta_2, c_2), (\eta_3, c_3)) \times \gamma_4(s \mid (\eta_4, c_4), (\eta_1, c_1), (\xi_3, -), (\xi_4, -)) \,. \quad (64)$$

The above-mentioned restrictions posed by γ_4 imply that the only nonzero term is that with $c_1 = c_4 = +$ and $c_2 = c_3 = -$, so this becomes

$$\int d\eta_1 \cdots d\eta_4 \, \{\boldsymbol{L}((\eta_1, +), (\eta_2, -), (\eta_3, -), (\eta_4, +)) f(s|\xi_1, \xi_2, \eta_2, \eta_3) f(s|\eta_4, \eta_1, \xi_3, \xi_4)\} \,. \quad (65)$$

The second and third terms can be similarly expressed in terms of f, using the antisymmetry of γ_4 and the charge-invariance properties. Using the relations

$$\begin{aligned} \boldsymbol{G}_s((\xi, +), (\xi', -)) &= -G_s(\xi', \xi), \\ \boldsymbol{G}_s((\xi, -), (\xi', +)) &= G_s(\xi, \xi'), \end{aligned} \quad (66)$$

and similarly for $\boldsymbol{S}_s$, we obtain

$$\dot{f}(s|\xi_1, \xi_2, \xi_3, \xi_4) = \Phi_{\rm pp}(s|\xi_1, \xi_2, \xi_3, \xi_4) + \Phi_{\rm ph}(s|\xi_1, \xi_2, \xi_3, \xi_4) - \Phi_{\rm ph}(s|\xi_1, \xi_2, \xi_4, \xi_3), \quad (67)$$

with

$$\Phi_{\rm pp}(s|\xi_1, \cdot\cdot, \xi_4) = \frac{1}{2} \int d\eta_1 \cdot\cdot d\eta_4 \, L(\eta_2, \eta_1, \eta_3, \eta_4) f(s|\xi_1, \xi_2, \eta_2, \eta_3) f(s \mid \eta_4, \eta_1, \xi_3, \xi_4) \quad (68)$$

and

$$\Phi_{\rm ph}(s|\xi_1, \cdot\cdot, \xi_4) = -\int d\eta_1 \cdot\cdot d\eta_4 \, L(\eta_1, \eta_2, \eta_3, \eta_4) f(s|\eta_4, \xi_2, \xi_3, \eta_1) f(s|\xi_1, \eta_2, \eta_3, \xi_4), \quad (69)$$

and where

$$L(\eta_1, \cdot\cdot, \eta_4) = S_s(\eta_1, \eta_2) G_s(\eta_3, \eta_4) + G_s(\eta_1, \eta_2) S_s(\eta_3, \eta_4) \,. \quad (70)$$

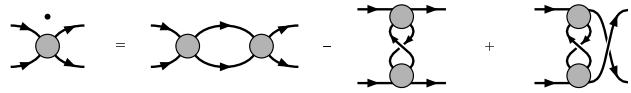

Fig. 2. The RGDE for f.

There is no $\frac{1}{2}$ in the expression for $\Phi_{\rm ph}$ because there are twice as many terms in the sum over intermediate charge indices c_i in the $\Phi_{\rm ph}$ as in $\Phi_{\rm pp}$. The function $\Phi_{\rm pp}$ is antisymmetric under exchange of (ξ_1, ξ_2) and of (ξ_3, ξ_4) because f has these properties. The function $\Phi_{\rm ph}$ is not antisymmetric, but the difference appearing in (67) is antisymmetric.

Equation (67) has the graphical representation shown in Fig. 2. The internal lines in these graphs correspond to "full" propagators G_s, and to single scale propagators S_s, respectively. The inverse of G_s is $g_2(s|\xi_1, \xi_2) = \gamma_2(s|(\xi_1, +), (\xi_2, -))$, and it satisfies

$$\dot{g}_2(s|\xi_1, \xi_2) = \dot{Q}_s(\xi_1, \xi_2) - \int d\xi_1\, d\xi_2\; S_s(\xi_4, \xi_3)\; f(s|\xi_1, \xi_3, \xi_4, \xi_2). \qquad (71)$$

4.2. *Spin rotation invariance*

We now derive the consequences of $SU(2)$-invariance (or, more generally, $SU(N)$-invariance).

The initial interaction of important many-fermion models has $SU(2)$ spin invariance. For instance, the initial Hubbard interaction, and interactions of the form $S_x \cdot S_y$, where $S_x = \bar{\psi}(x)\frac{\sigma}{2}\psi(x)$ is the spin at x, have this property. In the Gross-Neveu model, the interaction is $U(N)$-invariant for a model with N colors.

Restricting our consideration to 1PI vertex functions that have the same invariance excludes spontaneous symmetry breaking. In general this is a further assumption. But if the model is two dimensional, there is no true long-range order (LRO) in the system at any positive temperature, as demonstrated by the Mermin-Wagner theorem. (A version of this theorem applying to Hubbard models was proven by Koma and Tasaki.[8]) An effective action that is not invariant under $SU(2)$ spin rotations would automatically lead to LRO, and hence misleading results. Thus in two dimensions, the invariance is not an additional assumption, and it is very important to keep it in the effective interaction and the 1PI functions. The Kosterlitz-Thouless-like behaviour that is expected in two-dimensional superconductors below T_c is possible with spin-invariant interactions; they simply exhibit a slow power-law falloff. (In layered materials, there is always a coupling in the third direction which then stabilizes superconductivity.)

Spin rotation invariance restricts the form of f as follows. If we define a spin tensor (cf. (24))

$$F(s \mid x_1, \cdot\cdot, x_4)_{\sigma_1 \cdot\cdot \sigma_4} = f(s \mid (x_1, \sigma_1), \cdot\cdot, (x_4, \sigma_4)), \qquad (72)$$

then

$$F(s \mid x_1, \cdots, x_4) = -\varphi(s \mid x_1, x_2, x_3, x_4)D + \tilde{\varphi}(s \mid x_1, x_2, x_3, x_4)E, \quad (73)$$

where $D_{\sigma_1\cdots\sigma_4} = \delta_{\sigma_1\sigma_4}\delta_{\sigma_2\sigma_3}$ and $E_{\sigma_1\cdots\sigma_4} = \delta_{\sigma_1\sigma_3}\delta_{\sigma_2\sigma_4}$. This can be seen by the following argument (which also applies to $U(N)$-symmetries). The symmetry transforms the fields as $\psi \to U\psi$, $\bar{\psi} \to \bar{U}\bar{\psi}$. Considering an infinitesimal transformation, we see that the only invariants are given by the above products of Kronecker deltas, $E_{\sigma_1\cdots\sigma_n}$ and $D_{\sigma_1\cdots\sigma_n}$ (also in the $U(N)$ case).

The equation $E_{\sigma_2\sigma_1\sigma_3\sigma_4} = D_{\sigma_1\sigma_2\sigma_3\sigma_4}$ and the antisymmetry of f under $(x_1, \sigma_1) \leftrightarrow (x_2, \sigma_2)$ imply that

$$\begin{aligned}\tilde{\varphi}(s \mid x_1, x_2, x_3, x_4) &= \varphi(s \mid x_2, x_1, x_3, x_4) \\ &= \varphi(s \mid x_1, x_2, x_4, x_3). \end{aligned} \tag{74}$$

Making two exchanges of coordinates, we have (similarly to (74))

$$\varphi(s \mid x_2, x_1, x_4, x_3) = \varphi(s \mid x_1, x_2, x_3, x_4)\,. \tag{75}$$

However, there is no symmetry of φ under exchange of only one pair of coordinates.

That interactions of the form $S_x \cdot S_y$ can be written in the form (73) follows from the Fierz identity

$$\sum_{i=1}^{3} (\sigma^i)_{\mu\nu}(\sigma^i)_{\alpha\beta} = 2\delta_{\alpha\nu}\delta_{\beta\mu} - \delta_{\mu\nu}\delta_{\alpha\beta}. \tag{76}$$

Using (76), one can also reconstruct the four-fermion interaction in the form $\tilde{S}\cdot\tilde{S} + \tilde{\rho}\tilde{\rho}$, where $\tilde{S}$ transforms as a vector, and $\tilde{\rho}$ remains invariant, under global spin rotations. For general φ, the quantities $\tilde{S}$ and $\tilde{\rho}$ will not be local in space, but rather involve different points.

We now rewrite the RGDE in terms of φ. The spin sum in the particle-particle term is of the form

$$\sum_{\tau,\tau'} A_{\sigma_1\sigma_2\tau\tau'} B_{\tau'\tau\sigma_3\sigma_4} = (A * B)_{\sigma_1\sigma_2\sigma_3\sigma_4}, \tag{77}$$

and the spin sum in the particle-hole term is of the form

$$\sum_{\tau,\tau'} A_{\sigma_1\tau\tau'\sigma_4} B_{\tau'\sigma_2\sigma_3\tau} = (A \circ B)_{\sigma_1\sigma_2\sigma_3\sigma_4}, \tag{78}$$

where A and B represent F with different spatial arguments. A straightforward calculation gives the relations

$$\begin{aligned} &D * D = D, \quad D * E = E * D = E, \quad E * E = D, \\ &D \circ D = 2D, \quad D \circ E = E \circ D = D, \quad E \circ E = E\,. \end{aligned} \tag{79}$$

Inserting (73) into (67), using (79), and comparing the coefficient of $-D$, we get an RGDE in the form

$$\dot{\varphi}(s) = \mathcal{T}_{\rm pp}(s) + \mathcal{T}^{\rm d}_{\rm ph}(s) + \mathcal{T}^{\rm cr}_{\rm ph}(s), \tag{80}$$

where, using $\underline{x} = (x_1, x_2, x_3, x_4)$,

$$\mathcal{T}_{\rm pp}(s|\underline{x}) = -\int dy_1 \cdots dy_4 L(y_2, y_1, y_3, y_4)\varphi(s|x_1, x_2, y_2, y_3)\varphi(s|y_4, y_1, x_3, x_4), \tag{81}$$

$$\mathcal{T}^{\mathrm{d}}_{\mathrm{ph}}(s|\underline{x}) = -\int dy_1 \cdots dy_4 L(y_1,y_2,y_3,y_4)\Big[-2\varphi(s|y_2,x_2,x_3,y_3)\,\varphi(s|x_1,y_4,y_1,x_4) + \varphi(s|y_2,x_2,x_3,y_3)\,\varphi(s|y_4,x_1,y_1,x_4) + \varphi(s|x_2,y_2,x_3,y_3)\,\varphi(s|x_1,y_4,y_1,x_4)\Big], \tag{82}$$

$$\mathcal{T}^{\mathrm{cr}}_{\mathrm{ph}}(s|\underline{x}) = -\int dy_1 \cdots dy_4 L(y_1,y_2,y_3,y_4)\varphi(s|x_2,y_2,x_4,y_3)\,\varphi(s|y_4,x_1,y_1,x_3), \tag{83}$$

and $L(y_1,y_2,y_3,y_4) = S(y_1,y_2)G(y_3,y_4) + G(y_1,y_2)S(y_3,y_4)$. Similarly, the equation for the full inverse two-point function is

$$\dot{\gamma}_2(s|x_1,x_2) = \dot{q}_s(x_1,x_2) - \dot{\Sigma}_s(x_1,x_2), \tag{84}$$

with a scale-dependent self-energy Σ_s that satisfies

$$\dot{\Sigma}_s(x_1,x_2) = \int dx_3\,dx_4 S_s(x_4,x_3)\Big[\varphi(s|x_3,x_1,x_4,x_2) - 2\varphi(s|x_1,x_3,x_4,x_2)\Big]. \tag{85}$$

The initial condition for Σ_s depends on how the Fermi surface is renormalized.

Again, these equations have a convenient graphical interpretation: φ is the coefficient of the direct spin term D, where the spin of particle 1 is the same as that of particle 4, and similarly for 2 and 3. Thus we may draw the vertex as in Fig. 3, where the solid fermion lines going through the top and bottom of the vertex indicate that spin is conserved along these lines. The symmetry (75) implies that it does not matter if the vertex is drawn upside down. The contributions to the right-hand side of (80) can then be represented graphically as in Fig. 4. Thus (80) and (84) are obtained by the usual QED-like Feynman rules, and the factor 2 and the minus sign appear as the usual factors from the spin trace and the extra minus sign of the fermion loop.

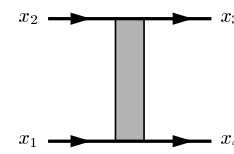

Fig. 3. The vertex corresponding to $\varphi(s|x_1,x_2,x_3,x_4)$.

Note, however, that this graphical correspondence does not mean that the fermion-boson vertex function that one can associate with the interaction by a Hubbard-Stratonovitch transformation is independent of momentum, as it would be for the bare Hubbard interaction. On the contrary, its momentum dependence is very important. Also, the propagators associated with the internal lines of these graphs are the full propagator $G(x,y)$ and the single-scale propagator $S(x,y)$. The function L is a symmetric combination of the two, which implies that every diagram stands for the two contributions given by the summands in L.

The symmetry (10) implies that

$$\varphi(s|x_1,x_2,x_3,x_4) = \overline{\varphi(s|Rx_4,Rx_3,Rx_2,Rx_1)}, \tag{86}$$

where $R(\tau,\boldsymbol{x}) = (-\tau,\boldsymbol{x})$. Similarly, the self-energy satisfies

$$\Sigma_s(x_1,x_2) = \overline{\Sigma_s(Rx_1,Rx_2)}. \tag{87}$$

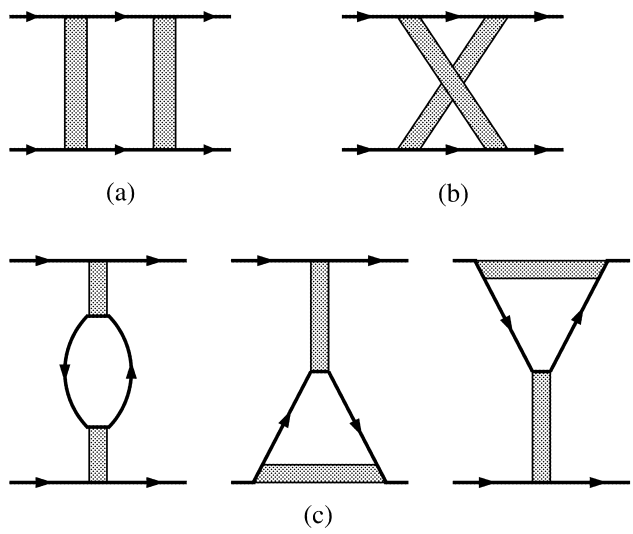

Fig. 4. The contributions to the right-hand side of the RGDE: (a) the particle-particle term; (b) the crossed particle-hole term; (c) the direct particle-hole term. The first of the three graphs gets a factor of -2, because of the fermion loop.

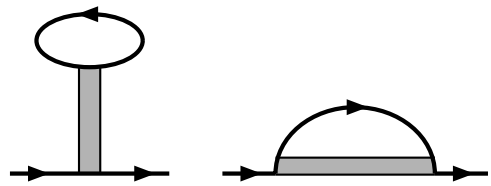

Fig. 5. The contributions to the self-energy.

The contributions to the right-hand side of (85) have the graphical representation shown in Fig. 5, where the internal line stands for a single scale propagator.

4.3. *Translation invariance*

If translation invariance is unbroken, we can take the Fourier transform. In contrast to charge and spin invariance, translation invariance is only discrete in our lattice model, and thus it may be broken at positive temperature also in two dimensions. Thus specializing to the case of unbroken translation invariance is a further assumption. It can be weakened if one assumes that invariance under a sufficiently large subgroup, e.g. that of translations of a sublattice, still holds. The corresponding Fourier transform is then defined on a smaller momentum space.

We use the convention in which momenta corresponding to $\bar{\psi}$ are counted as outgoing and those corresponding to ψ are counted as incoming. Then translational invariance implies that $\hat{\varphi}(s|p_1, p_2, p_3, p_4) = \delta(p_1 + p_2, p_3 + p_4)\, V_s(p_1, p_2, p_3)$, and the equation for V_s reads

$$\dot{V}_s = \hat{\mathcal{T}}_{\mathrm{pp}} + \hat{\mathcal{T}}^{\mathrm{d}}_{\mathrm{ph}} + \hat{\mathcal{T}}^{\mathrm{cr}}_{\mathrm{ph}}, \tag{88}$$

with the particle-particle term

$$\hat{\mathcal{T}}_{\rm pp}(p_1,p_2,p_3) = -\int dk \mathcal{L}_-(p_1+p_2,k) V_s(p_1,p_2,k) V_s(p_1+p_2-k,k,p_3), \quad (89)$$

the direct particle-hole term

$$\hat{\mathcal{T}}^{\rm d}_{\rm ph}(p_1,p_2,p_3) = -\int dk\ \mathcal{L}_+(p_2-p_3,k)\Big[-2V_s(k,p_2,p_3)\, V_s(p_1,p_2-p_3+k,k) + V_s(k,p_2,p_3)\, V_s(p_2-p_3+k,p_1,k) + V_s(p_2,k,p_3)\, V_s(p_1,p_2-p_3+k,k)\Big], \quad (90)$$

and the crossed particle-hole term

$$\hat{\mathcal{T}}^{\rm cr}_{\rm ph}(p_1,p_2,p_3) = -\int dk\ \mathcal{L}_+(p_3-p_1,k) V_s(p_2,k,p_1+p_2-p_3)\, V_s(p_3-p_1+k,p_1,k). \quad (91)$$

Here

$$\mathcal{L}_\pm(q,k) = \hat{S}(k)\hat{G}(q\pm k) + \hat{S}(q\pm k)\hat{G}(k). \quad (92)$$

The symmetry (86) implies that

$$V_s(p_1,p_2,p_3) = \overline{V_s(R(p_1+p_2-p_3), Rp_3, Rp_2)}, \quad (93)$$

with $R(\omega,\boldsymbol{p}) = (-\omega,\boldsymbol{p})$.

These RG equations were studied in Ref. 9), and similar ones are studied in Refs. 5) and 4). To allow for numerical solution, there are still too many variables. By projecting on the Fermi surface, one can reduce the number of variables in the equations. To calculate response functions, one then calculates the flow of susceptibility vertices, which is driven by that of the coupling functions. Details about the susceptibilities are given in the Appendix.

4.4. *Comparison to other RG schemes*

The main differences between this approach and that presented in Refs. 4) and 5) are the following. In Ref. 4), Polchinski's equation is used. The quantities appearing in that equation are the connected amputated Green functions, which are in general 1-particle reducible. Therefore, in the method of Zanchi and Schulz,[4] the tree-level six-point function must be kept and inserted into the equation for the four-point function, thereby yielding a flow equation that is nonlocal in the flow parameter ϵ_s. This is the normal procedure in integrating the flow equation, and, when iterated out, it gives a very useful representation for rigorous studies, first treated in Ref. 18). We note that in our truncation of the RGDE system, where we drop the *one-particle irreducible* six-point function from the flow, we also retain the one-particle reducible six-point function at tree-level. Thus, in this respect, the two formalisms are similar. However, in the 1PI formalism, the higher n-point functions are also all kept at tree level automatically, and the flow equation is local in s.

In Ref. 5), Halboth and Metzner use the Wick ordered RGDE of Ref. 2), which has a number of advantages. First, as in the 1PI scheme, the flow equation is

local; the influence of the six-point function on the four-point function is taken into account automatically by Wick ordering. The Wick ordering also implies that part of the lines are supported *below* the scale ϵ_s instead of above it. This makes the justification of projections to the Fermi surface easier, and it also leads to rather clear thresholds where scattering processes die out because the available phase space disappears. One disadvantage of the Wick ordered formalism is that taking self-energy corrections into account is not as convenient as in the 1PI formalism. If self-energy corrections are ignored, as done in Refs. 5) and 4), and mostly in Ref. 9), this disadvantage disappears. However, in the presence of van Hove singularities, self-energy corrections may be important. To this time, they have only been included in the calculation of the Fermi surface deformation reported in the appendix of Ref. 9).

§5. Geometric arguments for dropping the 1PI six-point function

In this section, we discuss the effects of the geometry of the energy shells which form the support of the single scale propagators on power counting. For the case of a smooth and curved Fermi surface, we use phase space bounds to estimate the contribution of the 1PI six-point function γ_6 to $\dot{\gamma}_4$. We show that in a specific scale range, the correction due to γ_6 is small even if the scale-dependent coupling constant is not small. We then discuss the case of Fermi surfaces with van Hove singularities.

5.1. *The term of order* $\gamma_4(s)^3$

We now focus on Fermi surfaces that are smooth and curved. We give this discussion for flow with a fixed Fermi surface. The Fermi surface deformation and the field strength renormalization can be dealt with using the methods of Refs. 11) and 12), and therefore not essential in this argument.

To estimate the influence of γ_6 on γ_4, we look at the integrated version of Eq. (53) for $\gamma^{(6)}$. This equation has the graphical representation shown in Fig. 6, where the m-legged vertex labelled by s represents $\gamma^{(m)}(s)$, and where we have also labelled the propagators associated with the lines. When the coefficients of the monomials in the fields are compared to obtain the corresponding equations for $\gamma_6(s|X_1, \cdots, X_6)$, the antisymmetrization condition implies that there is a sum over different possibilities of associating the internal propagators with the different lines, as in (60).

The vertex functions $\hat{\gamma}_m(s|p_1, \cdots, p_{m-1})$ have a natural power counting that is determined by the scaled propagator, or equivalently, the kinetic energy. To be specific, we choose a scaled propagator of the form

$$C_s(p) = \frac{1}{i\omega - e(\boldsymbol{p})}\, \chi\left(\frac{\omega^2 + e(\boldsymbol{p})^2}{{\epsilon_s}^2}\right), \tag{94}$$

where $\epsilon_s = \epsilon_0 e^{-s}$, with ϵ_0 some fixed energy scale, and where χ is a smooth and monotonically increasing cutoff function with $\chi(x) = 1$ for $x \geq 1$ and $\chi(x) = 0$ for $x \leq 1/4$. (The details of the choice of χ play no role in this argument.) The discussion of flows in which the cutoff function χ is frequency-independent (i.e. where $\chi(e(\boldsymbol{p})^2/{\epsilon_s}^2)$ is the cutoff function) is similar — the power counting is essentially the same.

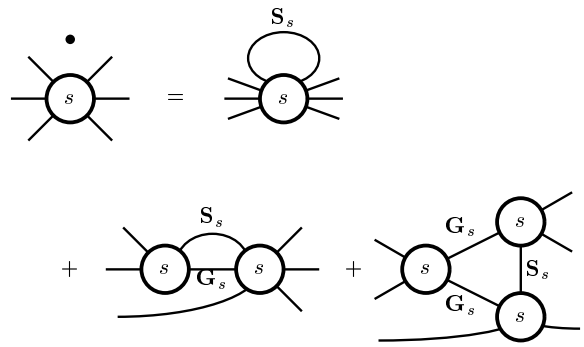

Fig. 6. The differential equation for $\gamma^{(6)}$.

The essential properties of $\dot{C}_s$ are that it is large near the Fermi surface, but zero outside a thin shell in $(d+1)$-dimensional momentum space around the Fermi surface. More precisely, because the differentiated cutoff function $\chi'(x)$ is nonzero only for $1/4 \le x \le 1$, the quantity $\dot{C}_s(k)$ vanishes unless $\epsilon_s/2 \le |i\omega - e(\boldsymbol{k})| \le \epsilon_s$, and hence

$$|\dot{C}_s(k)| \le \frac{2}{\epsilon_s} 1_s(k), \tag{95}$$

where 1_s is the indicator function $1_s(k) = 1$ if k is in the energy shell where $\dot{C}_s \neq 0$ (i.e. if $\epsilon_s/2 \le |i\omega - e(\boldsymbol{k})| \le \epsilon_s$), and $1_s(k) = 0$ if k is not in this shell. In terms of the density of states $N(E) = \int \frac{d^d\boldsymbol{k}}{(2\pi)^d}\, \delta(E - e(\boldsymbol{k}))$, the volume of this momentum space shell is

$$\begin{aligned} W(s) = \int d^{d+1}k\, 1_s(k) &\le \frac{1}{\beta} \sum_{|\omega| \le \epsilon_s} \int_{-\epsilon_s}^{\epsilon_s} dE\, N(E) \\ &\le A{\epsilon_s}^2, \end{aligned} \tag{96}$$

with the constant $A = \frac{2}{\pi} N_{\max}$, where $N_{\max}$ is the maximum of the density of states $N(E)$ over all energies satisfying $|E| \le \epsilon_s$. Because $N(E)$ is a surface integral over $1/|\nabla e|$, the constant A is finite only in absence of a van Hove singularity.

We integrate (53) from scale 0 to s. This gives, among others, the third order correction shown in Fig. 7 to $\dot{\gamma}^{(4)}(s)$. We consider this two-loop integral first and come back to the full equation for γ_6 below. Let $\gamma_4(s) = V_s$, and let

$$g(s) = \sup_{0 \le s' \le s} \sup_{p_1,p_2,p_3} |\gamma_4(s'|p_1, p_2, p_3)| \tag{97}$$

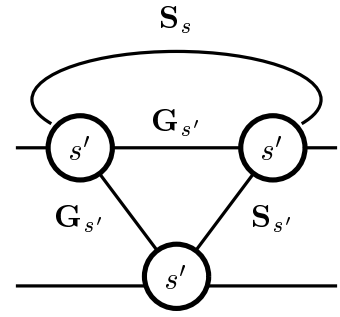

Fig. 7. A term cubic in γ_4 arising from the contribution of γ_6 to the flow of γ_4. This graph is integrated over s' from $s' = 0$ to $s' = s$.

be the maximal possible value of the four-point vertex at any flow time up to s (i.e. at energy scales satisfying $\epsilon_{s'} \geq \epsilon_s$), and for any values of the external momenta. The quantity $g(s)$ provides a bound for the largest possible four-point coupling constant that can arise in the flow. Because $g(s)$ is the maximum over $s' \leq s$, it is an increasing function of s. Because $g(s)$ includes the maximum over all momenta, we can bound all three vertex factors $\gamma_4(s')$ by $g(s')$. The contribution I_a of the graph in Fig. 7 is at most

$$I_a \leq \int_0^s ds' g(s')^3 \, J(s, s', q_1, q_2), \tag{98}$$

with

$$J(s, s', q_1, q_2) = \int dk \int dp \, |\boldsymbol{S}_{s'}(k) \boldsymbol{S}_s(p)| \, |\boldsymbol{G}_{s'}(\pm k \pm p + q_1) \boldsymbol{G}_{s'}(\pm k + q_2)|, \tag{99}$$

where q_1 and q_2 are linear combinations of the external momenta. They are unimportant, because our estimate of J is independent of q_1 and q_2. Because $g(s)$ is an increasing function of s, we can take it out of the integral to get

$$I_a \leq g(s)^3 \int_0^s ds' \, J(s, s', q_1, q_2). \tag{100}$$

The contribution is third order in $g(s)$. If $g(s)$ becomes large, it will only stay smaller than the second order terms if the coefficient function J is small. We next write

$$\boldsymbol{G}_{s'}(\pm k \pm p + q_1) = \int_0^{s'} ds'' \dot{\boldsymbol{G}}_{s''}(\pm k \pm p + q_1). \tag{101}$$

Because $\dot{\boldsymbol{S}}_s$ and $\dot{\boldsymbol{G}}_s$ have the same size and support properties as $\dot{C}_s$, we can use (95) to obtain

$$J(s, s', q_1, q_2) \leq \frac{1}{\epsilon_s {\epsilon_{s'}}^2} \int \frac{ds''}{\epsilon_{s''}} \, \mathrm{Vol}(s, s', s''), \tag{102}$$

with the two-loop momentum space volume

$$\mathrm{Vol}(s, s', s'') = \int d^{d+1}k \int d^{d+1}p \left\{ 1_s(p) \, 1_{s'}(k) 1_{s''}(\pm k \pm p + q_1) \right\}, \tag{103}$$

which depends on the three scales s, s' and s'' and on q_1. Here we have also used the fact that $1_{s'}(\pm k + q_2) \leq 1$, so that the dependence on q_2 has already dropped out. One can easily bound J by dropping the third indicator function from the integral. This gives

$$\mathrm{Vol}(s, s', s'') \leq W(s) W(s'), \tag{104}$$

with $W(s)$ as in (96). Hence, we have

$$J(s, s', q_1, q_2) \leq A^2 \epsilon_s \int_0^{s'} \frac{ds''}{\epsilon_{s''}}. \tag{105}$$

Because $\epsilon_s = \epsilon_0 e^{-s}$, the last integral is bounded by $1/\epsilon_{s'}$. Inserting this back into (100) and doing the integral over s', we arrive at the estimate

$$I_a \leq A^2 g(s)^3, \tag{106}$$

which does not suggest that this term is suppressed. This would correspond to usual power counting, which suggests that all four-legged contributions have the same order of magnitude.

However, if we do not drop $1_{s''}(\pm k \pm p + q_1)$ from the above integral, we obtain a better bound. It is shown in Refs. 11) and 12) (see also Appendix B.8 of Ref. 3)) that

$$\mathrm{Vol}(s, s', s'') \leq W(s)W(s')Q_{\mathrm{vol}}(1+s)\epsilon_{s''}, \tag{107}$$

where Q_{vol} is a constant that depends on the Fermi surface geometry and which we discuss below. This bound does not depend on q_1. For $d \geq 3$, the logarithmic factor $1+s$ is replaced by 1. Compared to (104), there is an extra factor $Q_{\mathrm{vol}}(1+s)\epsilon_{s''}$ in (107), and this factor is small for large s''. Integrating the scales in the same manner as above, we now obtain

$$I_a \leq A^2 Q_{\mathrm{vol}} g(s)^3 \epsilon_s (1+s)^2, \tag{108}$$

which, up to the factor $(1+s)^2$, is smaller by a factor of $\epsilon_s \sim e^{-s}$ than before.

Let us now calculate the correction that this gives. In the flow where the influence of γ_6 is omitted, we have

$$\dot{g}(s) \leq \tilde{\beta}_2 g(s)^2, \tag{109}$$

with $\tilde{\beta}_2 > 0$ the maximal value of the single-scale bubble integral. Here we have taken bounds, and this gives the worst case scenario. If one looks at the flow of a particular coupling constant (in an expansion in angular momentum couplings, e.g. the s-wave coupling), the sign of the coupling constant at $s = 0$ determines whether it grows or decreases under the flow. Taking the equality sign in (109), we find

$$g(s) = \frac{g(0)}{1 - g(0)\tilde{\beta}_2 s}, \tag{110}$$

which diverges at some nonzero s_c, indicating the possibility of instabilities. The flow given by (110) has essentially two different regimes. If $g(0)\tilde{\beta}_2 \ll 1$, then $g(s) \sim g(0) + g(0)^2\tilde{\beta}_2 s$ grows logarithmically in ϵ_s. When s approaches s_c, it starts to grow as the inverse power $1/(s_c - s)$.

At a positive temperature $T = 1/\beta$, the flow stops at $s_\beta = \log \frac{\beta\epsilon_0}{\pi}$, because nothing is left to integrate over when $\epsilon_s = \pi/\beta$. If $g(0)$ is so small that $s_c > s_\beta$, the four-point function remains finite, and there is no instability. This is the basis of the Fermi liquid criterion of Ref. 2): If $s_\beta \ll s_c$, the running coupling constants remain small and one can use convergent perturbation theory to justify Fermi liquid theory. However, even if the coupling constants do not remain small, the correction I_a to the $O(g(s)^2)$ four-point flow is small if

$$A^2 Q_{\mathrm{vol}} g(s) \epsilon_s (1+s)^2 \ll 1, \tag{111}$$

with $g(s)$ given by (110).

Thus the flow is naturally split into three different regimes:

(i) high scales, in which s is so small that $A^2 Q_{\mathrm{vol}} \epsilon_s (1+s)^2$ is not very small.

(ii) intermediate scales, in which s is such that (111) holds.

(iii) low scales, in which s is so large that (111) fails.

This provides a criterion to determine when the flow is accurate and when it has to be stopped, and it also makes clear what the role of weak coupling is in our treatment. A weak initial coupling constant is needed to get through regime (i) with a second order flow, because the only small factor in region (i) is the coupling $g(s)$. If the coupling constant is not weak, there can be significant corrections to the flow in this regime. In regime (ii), the coupling constant need not be small, because the scaling provides small factors that make the correction term small. In regime (iii), the corrections become dominant, so the one-loop flow has to be stopped before one enters regime (iii). What we expect to happen around this scale is that gaps open up that cut off the singularity.

If the initial interaction is sufficiently weak, or more precisely, if $g(0)\log\epsilon_0$ is sufficiently small, regimes (i) and (ii) will exist. This is because regime (i) is, by definition, the regime with infrared cutoff ϵ_0, and it has been proven [13] that perturbation theory for many-fermion systems converges, if there is an infrared cutoff. Thus, if the coupling constant is sufficiently small, low order perturbation theory can be used to calculate the effective interaction. After that, the truncated flow can be used in regime (ii). This flow decouples into angular momentum sectors (or their generalization in the absence of spherical symmetry; see, e.g., Ref. 10) or 3)) that flow independently. Coupling constants that start out positive will decrease to smaller positive values, and ones that start out negative will decrease to more negative values, and eventually, at some $\tilde{s}_c$, diverge in the one-loop flow. As discussed, there is no real divergence of coupling constants in the full flow; instead, one enters regime (iii), where the corrections to the one-loop flow can no longer be neglected.

It might happen that in the flow, all coupling constants remain positive. This would mean that none of them diverge. We do not know of any example for such behaviour for $d \geq 2$ and with $\boldsymbol{p} \to -\boldsymbol{p}$ symmetry: There is always a coupling constant that becomes negative (Kohn-Luttinger effect) at the scale ϵ_0, and therefore starts to grow in absolute value at lower scales. If the symmetry under $\boldsymbol{p} \to -\boldsymbol{p}$ is broken, there is no Cooper instability, and the coupling constants remain finite down to scale zero even at zero temperature. [15] The reason for this is not that all couplings remain positive (in fact, their sign does not matter), but that the constant $\tilde{\beta}_2$ is replaced essentially by const ${\epsilon_s}^{1/3}$ (see Lemma 4.8 in Ref. 12)), which just integrates to a constant, so that $g(s) \leq g(0)/(1 - g(0)\ \text{const})$ in this case.

5.2. *The influence of the full* γ_6

The above discussion is only for a single graph, but the essential points also apply to the other terms, due to the points we now discuss. The equation for γ_6 is linear. In finite volume, where the momenta are discrete, it can be viewed as a system of linear differential equations, labelled by $\underline{P} = (P_1, \cdots, P_6)$, where the P_i include momentum, spin, and charge indices. We have

$$\dot{\gamma}_6(s) = B_6(\gamma_4(s), \gamma_6(s)) + T_6(\gamma_4(s), \gamma_4(s), \gamma_4(s)) + L_6(\gamma_8(s)), \qquad (112)$$

where B_6, T_6 and L_6 are linear in each of the coupling functions, and depend on the momenta $\underline{P}$. We drop γ_8 from the equation. The argument for doing this is

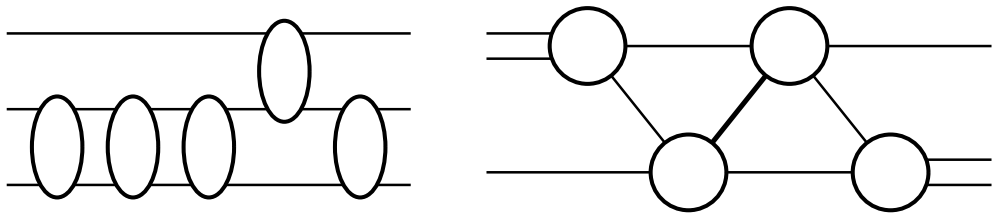

(a) (b)

Fig. 8. Graphical representation of terms arising in the solution of the differential equation for γ_6 as a function of γ_4: (a) a chain of four-legged insertions attached to the third-order term in the equation for γ_6; (b) a term containing overlapping loops which has a small scaling factor.

similar to the one that we are describing (see below). Now, γ_6 can be calculated in terms of γ_4 as a solution of the linear differential equation (112). Defining a maximal six-point coupling $g_6(s)$ (independent of momentum) in analogy to (97), we obtain

$$\dot{g}_6(s) \leq \tilde{\beta}_2 g(s) g_6(s) + \frac{1}{\epsilon_s} g(s)^3. \tag{113}$$

To get a bound for g_6, we replace the inequality by an equality. This is now just a linear differential equation in one variable s, which can be solved explicitly. Using the fact that $g(s)$ is increasing in s, we find

$$g_6(s) \leq \frac{1}{\epsilon_s} g(s)^3 \exp\left(\tilde{\beta}_2 \int_0^s g(s')\, ds'\right). \tag{114}$$

The main change in comparison with the discussion of the third order term is that the integral of $g(s)$ gets exponentiated. Using (110), we can calculate this integral, and we obtain

$$g_6(s) \leq \frac{1}{\epsilon_s} g(s)^3 \left(1 - g(0)\tilde{\beta}_2 s\right)^{-1}. \tag{115}$$

In other words, solving the differential equation for γ_6 gives another factor in the denominator which is similar to the one already in $g(s)$. Thus the power in the denominator increases by 1.

In graphical terms, the integration of the differential equation for γ_6 corresponds to a resummation of infinitely many graphs, and the new denominator comes from long chains of four-point functions attached to the third order term, as shown in Fig. 8 (a). These chains arise from iterating the same term in the equation many times.

The other terms, such as the one drawn in Fig. 8 (b), contain a loop overlap [11] on one line (e.g., the heavy line in the figure) and are therefore suppressed. (This is also the reason why the prefactor of $g(s)g_6(s)$ in (113) is $\tilde{\beta}_2$.) If one goes through this in more detail (which we skip here for brevity, and because the argument is similar to that in Ref. 11)), one finds that the overlapping loop structure is in all terms that do not involve self-contractions of four-point vertices. The latter are treated by a Fermi surface counterterm in the manner done in Refs. 11) and 12).

The backreaction of γ_6 on γ_4 is now obtained by joining two legs of different vertices to form an additional loop. The above discussion has shown that this always creates a loop overlap which cancels the factor of $1/\epsilon_s$ in (115). Hence the correction of γ_6 to the flow for γ_4 is bounded by

$$\psi(s, g(s)) = Q_{\mathrm{vol}} A^2 (1+s)^2 g(s)^3 \frac{1}{1 - g(0)\tilde{\beta}_2 s}. \tag{116}$$

Thus, the analogue of (111), with the power of the denominator increased by 1, defines the condition that the correction remains small.

The above argument has shown that, with $g(s)$ given by the unperturbed one-loop flow (110), the term $\psi(s, g(s))$ that we dropped is small in regions (i) and (ii). A standard stability analysis now shows that the solution of the equation where the contribution of γ_6 is taken into account in the equation for γ_4 is given by $g(s) \to g(s)(1 + h(s))$, where $h(s)$ is small as long as $\psi(s, g(s))$ remains small.

This completes the justification of dropping γ_6 in the equation for γ_4 under the hypothesis that γ_8 can be dropped from the equation for γ_6. We can now go on to discuss the equations for γ_8, etc. The same argument applies these, as can be seen by the following observations: (1) when γ_{m+2} is dropped, γ_m can be expressed in terms of γ_4 by integration of the differential equation; (2) the γ_m are 1PI functions, so the self-contraction term which γ_m contributes to γ_{m-2} always involves a two-loop graph which is either taken care of by Fermi surface renormalization or is multiplied by a small factor due to the overlapping loop bound. A careful graphical analysis is done in Refs. 11) and 12). The combinatorial problem is treated in Ref. 13).

5.3. *Fermi surfaces with van Hove singularities*

We now discuss the changes that result if van Hove singularities and a small curvature of the Fermi surface exist. Obviously, the estimate (96) for $W(s)$ no longer holds if the region of $\boldsymbol{k}$ satisfying $|e(\boldsymbol{k})| \leq \epsilon_s$ contains a zero of the gradient. For $d = 2$, the integral for $\boldsymbol{k}$ at a distance at most k_c from a saddle point of e is, in natural momentum space coordinates (u, v) around the saddle point, where $e(\boldsymbol{p}) = uv$,

$$\int\limits_{|e(\boldsymbol{k})| \leq \epsilon_s} \frac{d^d \boldsymbol{k}}{(2\pi)^d} \sim \int\limits_{\substack{|uv| \leq \epsilon_s \\ u^2 + v^2 \leq k_c^2}} du\, dv \sim \epsilon_s \log \frac{k_c^2}{\epsilon_s}, \tag{117}$$

and thus there is an extra logarithmic factor s. Again, for $d \geq 3$ this factor is replaced by 1. Moreover, Q_{vol} depends on the curvature of the Fermi surface and diverges if the curvature vanishes.

For our case, this implies that the argument for omitting higher order terms works only on those parts of the Fermi surface which are curved (and for which regime (i) can become uncomfortably large). Here, the assertion that the curvature is nonzero is meant in the more precise sense that the scale should be sufficiently low that $Q_{\mathrm{vol}}(1+s)\epsilon_s < 1$. Otherwise, (107) provides no improvement over (104). In the $t' = 0$ Hubbard model near half-filling (μ small), the improvement starts only at scales satisfying $\epsilon_s < \mu$. For the (t, t') model with $t' \neq 0$, the curvature

is nonvanishing away from the saddle points. Moreover, the curved region of the Fermi surface becomes larger and larger as the scale decreases, because the shells become thinner. Thus one can take the radius k_c of the disk around the van Hove singularity to shrink with ϵ_s, and the part of momentum space in which there is no improvement becomes smaller and smaller. Inside the disk of radius k_c, there is, however, no gain. Choosing k_c to be proportional to $\sqrt{\epsilon_s}$, we find that the influence of a region of that size to the integral is of order 1 instead of order s. Thus the origin of the extra logarithms is not in a very small neighbourhood of the van Hove singularity, but rather in the range $\sqrt{\epsilon_s} \leq k_c \leq 1$. This is similar to the fact that the one-dimensional integral $\int_0^1 \frac{dx}{\sqrt{x^2+a^2}}$, which grows as $|\log a|$ for small a, can be split into the contribution of a small neighbourhood of 0, $\int_0^a \frac{dx}{\sqrt{x^2+a^2}}$, which is bounded because it is no greater than $\int_0^a \frac{dx}{a} \leq 1$ and the piece $\int_a^1 \frac{dx}{\sqrt{x^2+a^2}} = \int_a^1 \frac{dx}{x} +$ regular terms, which produces the logarithm.

In presence of a van Hove singularity, the estimate of the leading flow, i.e. the largest coupling, changes to

$$g(s) = \frac{g(0)}{1 - g(0)\tilde{\beta} s^2}, \tag{118}$$

due to the extra logarithm from the local density of states integral (117), which effectively replaces $\tilde{\beta}_2$ by $\tilde{\beta}_2 s$ in the differential equation. The flow now diverges unless $T \geq T_0 e^{-1/\sqrt{g(0)\tilde{\beta}_2}}$, which is a much smaller value than in the absence of a van Hove singularity. It should be kept in mind, however, that in the weakly coupled repulsive Hubbard model, any attractive coupling generated by integrating out degrees of freedom is of order at least U^2, and therefore the square root just gives back the usual scaling of T as a function of U.

Acknowledgements

It is our pleasure to thank Gianni Blatter, Joel Feldman, Walter Metzner and Maurice Rice, for discussions.

Appendix A

—— Projections and Susceptibilities ——

Even the truncated system of RG equations cannot be solved exactly in physically interesting cases. The four-point function is a function of three momenta and three frequencies (the fourth being fixed by momentum conservation). Thus it is a function of $3d+3$ variables, and the RGDE is a nonlinear integro-differential equation for this function. Similarly, the self-energy depends on momentum and frequency. The large number of variables makes a computational solution of the RGDE difficult. However, the RG and its power counting provide further means for reducing the number of variables. The basic argument is, again, that the singularity is on the Fermi surface, and therefore only the degrees of freedom on the Fermi surface should influence the leading behaviour. A more detailed argument uses Taylor expansions

around the Fermi surface. Although often discussed as a standard RG argument, a rigorous justification of this procedure is nontrivial, in particular in the case with van Hove singularities.

The projected four-point function no longer contains all of the information, and, in particular, it is not sufficient for calculating response functions to determine instabilities. These response functions can be recovered by considering a flow with external fields and calculating the linear and quadratic term in the external field.

The general features of these equations are that only the equation for the coupling function (i.e. the projected function) is nonlinear, and that, given the coupling function, the others can be obtained from a linear equation whose coefficients depend on the coupling function. In this way, the logarithmic growth of couplings integrates to imply power laws of the response functions. This is also the case for the four-point function away from the Fermi surface.

The susceptibilities are obtained by coupling external boson fields a to the bilinears in the fermions that represent charge, spin, Cooper pairs and other local densities, and by calculating the corresponding RG flow for these functions. The presence of the a fields has no role in the derivation of the RGDE, because the a fields simply appear as parameters. Thus the equations are unchanged, except that now all functions depend on a. The fields a are external, because no integration over a is done. Correlation functions for the gaps, spins, etc., are given by derivatives of the generating functional with respect to the a fields. Thus for their calculation, it suffices to obtain the dependence on a in terms of an expansion in a. The expansion of Γ_s now reads

$$\Gamma(s \mid a, \phi) = \sum_{m,n \geq 0} \gamma^{(m,n)}(s \mid a, \phi), \tag{119}$$

with

$$\gamma^{(m,n)}(s \mid a, \phi) = \frac{1}{m!n!} \int d^m \underline{X}\, d^n \underline{Y} \gamma_{m,n}(s|\underline{X}, \underline{Y}) a^m(\underline{X}) \phi^n(\underline{Y}) \,. \tag{120}$$

Because the a fields are boson fields, the coefficient $g_{m,n}(s|\underline{X}, \underline{Y})$ is totally symmetric under permutations of $\underline{X}$. The RGDE can now be derived in the same manner as above. Because the a fields are external fields only, the equations for the a-independent parts γ_{0n} remain unchanged, so that $\gamma_{0n} = \gamma_n$ for all n, with the γ_n given as above. Thus the flow for the susceptibilities is driven by the flow for the coupling functions; it takes the form of a system of linear integro-differential equations.

For $m + n > 0$, we have

$$\begin{aligned} \dot{\gamma}^{(m,n)}(s \mid a, \phi) = &-\frac{1}{2} \operatorname{Tr} \left[G_2 \dot{\boldsymbol{Q}}_s G_2 \tilde{\gamma}^{(m,n)}(s \mid a, \phi) \right] \\ &+ \frac{1}{2} \sum_{p \geq 2} (-1)^p \left\{ \sum_{\substack{m_1, \cdots, m_p \geq 0 \\ m_1 + \cdots + m_p = m}} \sum_{\substack{n_1, \cdots, n_p \geq 2 \\ n_1 + \cdots + n_p = n}} \operatorname{Tr} \left[G_2 \dot{\boldsymbol{Q}}_s \prod_{q=1}^{p} G_2 \tilde{\gamma}^{(m_q, n_q)}(s \mid a, \phi) \right] \right\}, \end{aligned} \tag{121}$$

with $\tilde{\gamma}^{(m,n)}$ defined in analogy to (44) and (45).

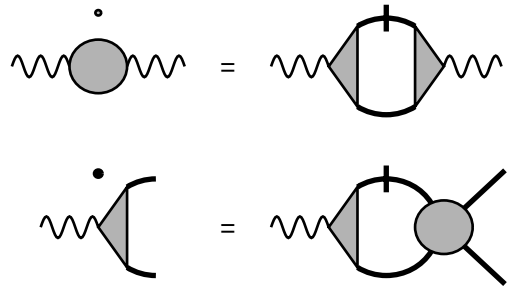

Fig. 9. The differential equations for γ_{20} and γ_{12}.

Since one a field couples to a fermionic bilinear, an external a field corresponds to a pair of fermions. Thus the truncation consistent with dropping the 1PI six-point function consists of leaving out all m and n with $2m + n \geq 6$. This gives the equations

$$\dot{\gamma}_{12}(s|X;Y_1,Y_2) = \frac{1}{2}\int d^4\underline{Z}\Big\{\boldsymbol{L}(Z_1,\cdots,Z_4)\gamma_{12}(s|X,Z_2,Z_3)\gamma_{04}(s|Z_4,Z_1;Y_1,Y_2)\Big\} \tag{122}$$

and

$$\dot{\gamma}_{20}(s|X_1,X_2) = \frac{1}{2}\int d^4\underline{Z}\Big\{\boldsymbol{L}(Z_1,\cdots,Z_4)\gamma_{12}(s|X_1,Z_2,Z_3)\gamma_{12}(s|X_2;Z_4,Z_1)\Big\}, \tag{123}$$

with $\boldsymbol{L}$ given by (60). The initial condition on γ_{12} at $s = 0$ determines which susceptibility is considered. In particular, it determines the symmetry of the superconducting instability in the case of the coupling to Cooper pairs.

In the presence of charge invariance, we get separate equations for the particle-particle ("superconductance") and particle-hole ("normal") susceptibilities, defined as

$$\gamma_{12}^{\mathrm{pp},\epsilon}(s|X,(y_1,\sigma_1),(y_2,\sigma_2)) = \gamma_{12}(s|X;(y_1,\sigma_1,\epsilon),(y_2,\sigma_2,\epsilon)) \tag{124}$$

and

$$\gamma_{12}^{\mathrm{ph},\epsilon}(s|X,(y_1,\sigma_1),(y_2,\sigma_2)) = \gamma_{12}(s|X;(y_1,\sigma_1,\epsilon),(y_2,\sigma_2,-\epsilon)). \tag{125}$$

By the fermionic antisymmetry, we have

$$\gamma_{12}^{\mathrm{pp},-}(s|X,(y_1,\sigma_1),(y_2,\sigma_2)) = -\gamma_{12}^{\mathrm{pp},+}(s|X,(y_2,\sigma_2),(y_1,\sigma_1)), \tag{126}$$

and similarly for $\gamma_{12}^{\mathrm{ph},\pm}$. Thus it suffices to consider either the + case or − case. We now also assume spin rotation invariance. Then the normal charge ($\sim \delta_{\sigma_1\sigma_2}$) and

spin susceptibility, $\sim (\tau_3)_{\sigma_1\sigma_2}$ (where τ_3 is the Pauli matrix), do not couple in the flow. The resulting equations are

$$\dot{\gamma}_{12}^{\mathrm{pp},-}(s|X,(y_1,\sigma_1),(y_2,\sigma_2)) = \int du_1 \cdots du_4 \Big\{ L(u_1,\cdots,u_4)\gamma_{12}^{\mathrm{pp},-}(s|X,(u_2,\sigma_1),(u_3,\sigma_2))\,\varphi(s|u_4,u_1;y_1,y_2)\Big\} \tag{127}$$

for the superconductance susceptibility,

$$\dot{\gamma}_{12,\mathrm{charge}}(s|x;y_1,y_2) = \int du_1 \cdots du_4 \Big\{ \mathrm{Re}\; L(u_1,u_2,u_4,u_3) \gamma_{12,\mathrm{charge}}(s|x;u_3,u_2)\,[2\varphi(s|y_1,u_1,u_4,y_2) - \varphi(s|u_1,y_1,u_4,y_2)] \Big\} \tag{128}$$

for the charge susceptibility, and

$$\dot{\gamma}_{12,\mathrm{spin}}(s|x;y_1,y_2) = \int du_1 \cdots du_4 \Big\{ \mathrm{Re}\; L(u_1,u_2,u_4,u_3)\gamma_{12,\mathrm{spin}}(s|x;u_1,u_4)\varphi(s|u_3,y_1,u_2,y_2)\Big\} \tag{129}$$

for the spin susceptibility.

References

1) J. W. Negele and H. Orland, *Quantum Many-Particle Systems* (Addison-Wesley, Reading, MA, 1988).
2) M. Salmhofer, Commun. Math. Phys. **194** (1999), 249.
3) M. Salmhofer, *Renormalization, Springer Texts and Monographs in Physics* (Springer, Heidelberg, 1998).
4) D. Zanchi and H. J. Schulz, Phys. Rev. **B61** (2000), 13609.
5) C. Halboth and W. Metzner, Phys. Rev. **B61** (2000), 7364.
6) J. Polchinski, Nucl. Phys. **B231** (1984), 269.
7) B. Simon, *The Statistical Mechanics of Lattice Gases, Volume 1* (Princeton University Press, Princeton, NJ, 1993).
8) T. Koma and H. Tasaki, Phys. Rev. Lett. **68** (1992), 2348.
9) C. Honerkamp, M. Salmhofer, N. Furukawa and T. M. Rice, cond-mat/9912358, to appear in Phys. Rev. **B63** (2001).
10) J. Feldman and E. Trubowitz, Helv. Phys. Acta **63** (1990), 157; **64** (1991), 213.
11) J. Feldman, M. Salmhofer and E. Trubowitz, J. Stat. Phys. **84** (1996), 1209.
12) J. Feldman, M. Salmhofer and E. Trubowitz, Comm. Pure Appl. Math. **51** (1998), 1133; **52** (1999), 273; **53** (2000), 1350.
13) J. Feldman, J. Magnen, V. Rivasseau and E. Trubowitz, Helv. Phys. Acta **65** (1992), 679.
14) M. Salmhofer, Rev. Math. Phys. **10** (1998), 553.
15) J. Feldman, H. Knörrer, D. Lehmann and E. Trubowitz, in *Constructive Physics*, ed. V. Rivasseau (Springer Lecture Notes in Physics, 1995).
16) N. Furukawa, T. M. Rice and M. Salmhofer, Phys. Rev. Lett. **81** (1998), 3195.

17) M. Disertori and V. Rivasseau, cond-mat/9907130.
18) D. C. Brydges and T. Kennedy, J. Stat. Phys. **48** (1987), 19.
19) M. Randeria et al., Phys. Rev. Lett. **74** (1995), 4951.
J. C. Campuzano et al., Phys. Rev. **B52** (1995), 615.